ISAS - INTERNATIONAL SCHOOL FOR ADVANCED STUDIES

Tersoff Potential For Semiconductors : Bulk, Defects and Surface Properties

Thesis submitted for the degree of

"Magister Philosophiæ"

CANDIDATE

Jorge Jair Botina P.

SUPERVISORS

Prof. Stefano Baroni

Dr. Furio Ercolessi

October 1990

TRIESTE

SISSA - SCUOLA INTERNAZIONALE SUPERIORE DI STUDI AVANZATI

TRIESTE

Strada Costiera 11

Scuola Internazionale Superiore di Studi Avanzati

International School for Advanced Studies

Tersoff Potential for Semiconductors : Bulk, Defects and Surface Properties

Thesis submitted for the degree of

"Magister Philosophiæ"

CANDIDATE

Jorge Jair Botina P.

SUPERVISORS

Prof. Stefano Baroni

Dr. Furio Ercolessi

Academic year 1989/90

Index

Desidero ringraziare la famiglia Martino che mi ha dato la possibilita di conoscere da vicino l'Italia ed uno dei suoi volti ed in particolare Giusy.

Acknowledgements

I would like to express my gratitude to Professors Furio Ercolessi and Stefano Baroni for their support and the chance they gave me to know about this subject, in particular I thank Furio Ercolessi for his help.

I want to thank also Dr. Pasquale Pavone for his contribution to the esthetical part and the study of phonon spectrum.

Especially I remember the fruitful talks with Dr. Enrico Smargiassi about point defects and with Prof. Annabella Selloni about the study of surfaces.

Chapter 1

Introduction

In recent years, with the increasing availability of powerful computers, it has been frequently demostrared that numerical methods play a very important role in condensed matter physics. One of the most successful applications of computes to the study of many–particle systems has been molecular dynamics. Based on the existence of a model that, given the atomic positions, allows to calculate the forces acting on them as a result of the mutual interactions, the molecular dynamics method uses a computer to integrate the Newton's equations and follow the time evolutin of the system. This allows to study structural, dynamical and thermodynamical properties of many–particle systems even in low–symmetry configurations, which is of course impossible to achieve by analytical methods.

The most crucial ingredient in molecualr dynamics is the force model. In fact, forces on the atoms are the result of very complex, many body interactions between all the electrons and the nuclei in the system. Almost invariably, force models attempt to circumvent the complexity of the real world by using some cleverly chosen empirical or semiempirical analytic form. This form tries to mimick the potential energy surface in configuration space of the real system by dealing only with the atomic coordinates. However, for certain classes of materials such as metals or semiconductors, choosing a realistic force model is certainly a non–trivial task.

Recently, a leap forward in this direction has been made by the Car–Parrinello method[1], based on the combination of the DFT with molecular dynamics simu-

lation. This method gives the chance to describe the dynamics of the ions (still treated as classical particles) under the action of forces generated directly from the ground state electron energy according to the Born–Oppenheimer approximation. In other words, with this approach the structure and dynamical properties at finite temperature become accessible by first principle calculations. Despite the great improvement obtained over empirical methods, it remains practically impossible to treat more complex systems, involving a large number of particles, as required to simulate e.g. molecular beam epitaxy or solid phase crystal growth of amorphous interfaces because of the huge amount of computer resources that would be necessary. Therefore, research in empirical potentials is still worth to be pursued, since they are likely to coexist with first–principle schemes, at least for some time.

Semiconductors are perhaps the most widely studied materials, due to their key position in technological applications. But they are also among the most difficult to model with a classical potential. The tetravalent character gives rise to the diamond structure, which requires the presence of at least 3–body terms to be accounted for. Early approaches in this direction, reviewed in the firts chapter, were somewhat unsatisfactory, in that only some physical properties could be reproduced correctly, while others (such as SW potential doesnot reproduced the the structural phase transition) turned out to be difficult to obtain.

More recently, Tersoff[2] introduced a many–body term which greatly improves the physical description, and produced a family of potentials based on this formulation. In particular, Tersoff poptentials are available for Si[3], Ge[2], C[4] and multicomponent[2] systems such as SiC and SiGe.

In this thesis, I discuss the implementation of these potentials in a molecular dynamics program, and present some results obtained. The work is organized in the following way:

In the second chapter you find a general description of semiempirical potentials for semiconductors, focusing on the role played by bond order and a description of Tersoff potential.

In the thirst chapter we make a presentation of the crystal properties calculated, using the Tersoff potential, namely cohesion energy, lattice parameter, elastic constants, bulk modulus, crystal stability, phonon and density of states. Our results are compared with previous calculations in the local density approximation.

In the last two chapters we present the results of static calculations on point defects such as vacancy, split vacancy, and two interstitial point defects (in tetrahedral and in hexagonal sites), and an anlysis of the migration of a vacancy. We also study the surface structure of the (100) and (111) surfaces of Si,Ge and C.

Chapter 2

Tersoff Potential

The knowledge of the total energy of a system of atoms as a function of the atomic coordinates is very important in the study of a lot of problems in physics, chemistry and material science. In fact, an analytical or an easily evaluable numerical expression of the total energy allows the application to large systems of methods which provide an accurate description of both static and dynamic properties. Among these methods we find molecular dynamics and global search for the energy minimum. These are purely classical methods and permit to study a lot of problems such as melting, surface reconstruction, crystal growth, amorphous structures, diffusion barrier and atomic clusters.

Furthermore, the knowledge of the potential $V(\mathbf{R})$ allows us to evaluate both the total energy E of a set of N particles as function of the particles coordinates $\{\mathbf{R}_i\}$ $\quad i = 1, ..., N$, and to calculate the force acting on the particles in any configuration. If the calculation of this function does not present any difficulties and if it provides a sufficiently accurate description of the physics of the system, realistic calculations of the properties of quite large systems and even of statistical ensembles are possible. This kind of approach provides a description of the system which is obviously less accurate than that of the modern *ab–initio* calculations, but it is in principle simpler to apply.

a.) Classical Interatomic Potentials

Most of the empirical interatomic potentials fall into two simple groups. One group consists of pair potentials, among these we cite the "famous" Lennard–Jones 6–12 and the exponential Morse potentials. However, for covalent materials, such as semiconductors, the pair potentials alone are inadequate, as an example the equilibrium diamond lattice is unstable relatively to close packed structures in absence of three body interaction.

The other group of potentials is constructed expanding the potential energy of a system in terms of the atomic displacements around some reference structure (in the case of semiconductors the diamond structure is often chosen). In this class for example the potential found by Keating has had a great success in describing local distortions and phonons[5]. However, they fail in describing the energy of structures which differ qualitatively from the reference one. These type of potentials[6] are of perturbational nature, therefore cannot be applied in a proper way to systems where the "difference" with the reference is not "small", such as systems with defects, surfaces and systems near the melting.

Of these two approaches, the pair potential takes advantage of a somewhat differentiation expansion.

Let us consider a system containing N atoms, then the potential energy E may be separated into terms depending on the coordinates of individual atoms, pairs, triplets,...:

$$E = \sum_i V_1(\mathbf{R}_i) + \sum_i \sum_{j>i} V_2(\mathbf{R}_i, \mathbf{R}_j) + \sum_i \sum_{j>i} \sum_{k>i>j} V_3(\mathbf{R}_i, \mathbf{R}_j, \mathbf{R}_k) + \ldots \quad (2.1)$$

where $\mathbf{R}_n$ is the position of n-th particle and the function V_m represents the so called "m-body potential". The first (one body) term, $V_1(\mathbf{R}_i)$, expresses the effects of an external potential on the system. The remaining terms represent

particular interactions. In the second term, the pair potential V_2 depends only on the magnitude of pair separation $R_{ij} = |\mathbf{R}_i - \mathbf{R}_j|$, so that it may be written as $V_2(R_{ij})$. Then the V_3 term involves triplets of atoms and so on for the other terms. Within the purpose of overcoming the inadequacy of pairwise (two body) potentials in the description of covalent systems, it is natural to retain terms up to the third in the expansion (2.1). The additional term permits to stabilize open structures with respect to close–packed ones, for example for semiconductors by favoring bond angles corresponding to those of the diamond structure.

The first attempt in such a direction was made by Person, Takai, *et al.* (PTHT)[7]. They used the nonseparable Acilrod–Teller three–body potential[8] which is based on the generalization of Vann der Waals fluctuating-dipole forces for three particles. The latter potential is long ranged (decaying as $V_3 = \frac{1}{R^9}$). The parameters in this potential were obtained through an average fit to the bond lengths and cohesive energies of bulk diamond Si and molecular Si_2.

The PTHT potential does not predict reasonable elastic properties for bulk silicon or its high-pressure polymorphous structure, but it fits small clusters fairly well and fits the experimental phase transition from the diamond structure to the β–tin structure quite well.

On the contrary, Stillinger and Weber[9] (SW) proposed a new empirical interatomic potential, incorporating a two and a three body interaction, and used it in molecular-dynamics simulations of molten silicon. They used the Lennard–Jones pairwise potential and included a term in the three body potential which favours the ideal tetragonal structure. A particular aspect of the model is that it is a short-range one, confined to two neighbour shells where the angular variation of the three body potential has a Keating type form. Studies using the SW potential have indicated that it reproduces the elastic properties of bulk silicon, but that

it does not handle some surface structures, low-coordinate number geometries, or high-pressures polymorphous properly[10]. Other physical aspects studied are the melting point of silicon[9], faceting at the (100) crystal melt interface[11], and the stability of coherently strains SiGe layer on an Si(111) substrate[12]. Biswas and Hamann[13] have criticized this potential, noting that it does not describe even qualitatively the behaviour of non–tetragonal polytypes of silicon.

An improved class of empirical potentials for silicon and other covalently bonded semiconductors is based loosely on ideas from quantum chemistry and observations concerning the universality of mechanical behaviour of solids[14,15]. The essential idea here, introduced first by Abell[16], is that the bonding can be properly described by pairwise interactions (for which a Morse–type potential is a reasonable approximation), but whose strength is influenced by the local environment, e.g., by many-body interference terms. This picture of covalent bonding was, apparently independently, developed and implemented by Biswas and Hamann who constructed two different potentials for silicon[13,17]. The two classical interatomic potentials express the environment near the pair bond by expansion in Legendre polynomials, which are then used to modify a generalized Morse potential. The three body potential is then fit to the density-functional theory structural data base for silicon[18]. One potential models bulk energies, high-pressure and simple structure properties very well, the other one is more appropriated for properties of the tetrahedral structure and useful in molecular-dynamics simulation of amorphous-Si structures and crystal growth processes such as molecular beam epitaxial[19] or the solid phase epitaxial growth of a crystal amorphous interface.

Biswas and Hamann suggest that a three body potential is not adequate for describing accurately the cohesive energy of silicon over a wide range of bonding geometry and coordination. This is a motivation for Tersoff to develop a new

potential, not taking into consideration the idea of the N-body potential and developing a pairwise potential including the many body terms in it. The new potential is made for C, Si, Ge, SiC and SiGe. With this type of potential he studied elastic constants, coordination numbers, bulk properties for Si[3], C[4], SiC[2] and alloys with SiGe[20], also the liquid and amorphous Si[21], C[4]. Dadson modified the initial potential stabilizing the diamond structure for the silicon[22].

Bolding and Andersen[23] developed an interatomic potential for silicon where the potential has the general form developed by Tersoff[3] with the interaction between a pair of atoms being dependent on the environment around them. The atom–atom potential energy function is expressed as a sum of π and σ bonding terms, each independently influenced by the environment. This potential is confined within a two neighbour shell. This potential gives a very good description of the structural phase transition, phonons, surface reconstructions and clusters[23].

Other types of models of potentials have been proposed: The thermal classical force field (CFF)proposed by Chelikowsky, Phillips, Kamal, Straus (CPKM)[24] and Wang,Messmer[25]. In some cases these agree with the $ab - initio$ geometries for the cluster but do not reproduce the energetic very well. The CPKM thermodynamic interatomic force field seems the most promising of these and has recently been applied to silicon clusters[26]. It has not been tested for surface properties or crystal defects.

Khor and Das Sarma[27] have developed a flexible analytic potential for silicon that seems promising. Unfortunately it uses a slightly different functional form and parameter set modeling the surface and bulk behaviour.

Baskes[28] proposed a potential based upon a modification of the embedded-atom method[29]. This resulted to be extremely powerful in modelingFCC metals but how will it represent covalent systems has yet to be determined.

The panorama of the classical potentials for semiconductors is wonderful and open to further studies. In fact for instance extremely good results were obtained in the field of metals where the empirical potential permitted to get to precise description of the physical properties. But if we think about semiconductors they are different because the deep links between the various elements and their diversity represented an obstacle for reaching efficient results. That is why it is necessary to go on developing the properties and possibilities of empirical potentials in order to obtain results which are closer to the reality and as much precise as possible. In a few words, a lot has been done but the possibilities still totally unexploited, are enormous.

b.) Modeling the chemical bonding

Which considerations are important for the construction of a classical interatomic potential? How can we express the energy of each atom in terms of the positions of the other atoms? The most important property is the nature of the bonds between atoms, which is of prime importance to understand the differences in the gross structure and the characteristics of different solids.

To model the chemical bonding, one important variable to consider is the number of neighbour atoms close enough to form bonds,i.e. the number of coordination. We remember in fact that for different materials or structures the local atomic coordination changes. For example in molecular bonding the interaction among very few atoms is extremely strong. It also important to consider the closeness of the atoms. As a matter of fact it is known that the influence of an atom far from the one we are studying is very small. An other aspect to be underlined is that the more neighbours the atom has, the weaker the bond to each neighbour

will be. In addition for covalent materials between bonds also play a crucial role.

All these considerations lead to the conclusion that the geometry is the key element for determining the bond strength. In practially all cases except perhaps rare gases, the pair potential alone is clearly inadequate. Therefore one has to include many–body interaction terms in the total potential energy. In this way it is possible to stabilize more open structures,such as the diamond structure for covalent materials, not possible to obtain by pairwise potentials. In the following section, some model Hamiltonians for semiconductors are presented.

c.) Tersoff Potential for Semiconductors

First of all it is necessary to remember the extreme importance of the bond order in the field of semiconductors and the role it plays. Biswas and Hamann[17] suggested the addition of a three–body term to the two body potential. But for covalent materials no good results were obtained and the final descriptions were not sufficiently precise. The proposition also of a four– or five–body potential for the calculation would probably have proved intractable. Tersoff had instead a brilliant new idea: the inclusion of a many–body terms *into* a two–body potential.

In the Tersoff[2] scheme, it is assumed that the total potential energy E of interaction among a collection of N atoms could be written as a sum of environment dependent pair potentials:

$$E = \sum_i E_i = \frac{1}{2} \sum_{i \neq j} V_{ij} \tag{2.2}$$

The interatomic potential between two atoms is taken to be of the form

$$V_{ij} = f_C(R_{ij})[f_R(R_{ij}) + b_{ij} f_A(R_{ij})] \tag{2.3}$$

where f_R and f_A represent the repulsive and attractive parts of the potential energy, f_C is a cutoff function for the interaction and b_{ij} is a many body term that includes the effect of the environment on the (i,j) bond. For f_R and f_A Tersoff uses the two exponential terms in a Morse potential, which have the very desirable feature of leading automatically to the "universal" behaviour discussed by Ferrante, Smith and Rose[14]. The form of these functions is given as:

$$f_R(R_{ij}) = A_{ij}\exp(-\lambda_{ij} R_{ij}) \tag{2.4.a}$$

$$f_A(R_{ij}) = -B_{ij}\exp(-\mu_{ij} R_{ij}) \tag{2.4.b}$$

and the cutoff function f_C as

$$f_C(R_{ij}) = \begin{cases} 1, & \text{if } R_{ij} < rij \\ \frac{1}{2} + \frac{1}{2}\cos[\pi(R_{ij} - r_{ij})/(S_{ij} - r_{ij})], & \text{if } r_{ij} < R_{ij} < S_{ij}, \\ 0, & \text{if } R_{ij} > S_{ij}; \end{cases} \tag{2.4.c}$$

which has continuous values together with its derivative for all R, and goes from 0 to 1 smoothly. The value of the parameter S_{ij} is chosen by limiting the interactions to the first neighbour shell only, reflecting the short–range character of forces in semiconductors, where i, j represents particular components.

For the environment term b_{ij}, Tersoff chooses

$$b_{ij} = \chi_{ij}(1 + \beta_i^{n_i}\zeta_{ij}^{n_i})^{-1/2n_i} \tag{2.4.d}$$

where ζ_{ij} is a function of the environment of atom i. As a consequence, b_{ij} is a function of the environment of the ij bond. The function ζ_{ij} is given by:

$$\zeta_{ij} = \sum_{k \neq i,j} f_C(R_{ik})\omega_{ij} g(\theta_{ijk}) \tag{2.5.a}$$

where

$$g(\theta_{ijk}) = 1 + \frac{c_i^2}{d_i^2} - \frac{c_i^2}{d_i^2 + (h_i - \cos\theta_{ijk})^2} \qquad (2.5.b)$$

where θ_{ijk} is the bond angle between bonds ij and ik. $g(\theta_{ijk})$ models the many–body interactions about one s pecified particle i. ω_{ij} was taken to be $exp(-\lambda_3^3(R_{ij} - R_{ik})^3)$ in the first versions of the potential[3], where λ_3 is a new parameter, and i, j, k are diferent between them. While $\omega_{ij} = 1$ is chosen in the most recent ones[2]. For simple materials like silicon, germanium, carbon, all parameters in the potential are chosen primarily by fitting the cohesive energy and bulk modulus in diamond structure. The values of these parameters for simple elements are given in the table 1.1. For multicomponent systems such as SiC and SiGe the new parameters for these mixtures are presented as follows, where a new constant χ given in the stoichometric relation of the mixture appears:

$$\lambda_{ij} = (\lambda_i + \lambda_j)/2, \qquad \mu_{ij} = (\mu_i + \mu_j)/2, \qquad A_{ij} = (A_i A_j)^{1/2},$$

$$B_{ij} = (B_i B_j)^{1/2}, \qquad r_{ij} = (r_i r_j)^{1/2}, \qquad S_{ij} = (S_i S_j)^{1/2}$$

In these parameters, the subscript i, j depend only on the type of atom (C,Si or Ge).

TAB. 1.1: Parameters for carbon, silicon and germanium to be used in eq.(2).

	C	Si	Ge
A(eV)	1.3936×10^{3}	1.8308×10^{3}	1.769×10^{3}
B(eV)	3.467×10^{2}	4.7118×10^{2}	4.1923×10^{2}
$\lambda(\AA)$	3.4879	2.4799	2.4451
$\mu(\AA)$	2.2119	1.7322	1.7047
β	1.5724×10^{-7}	1.10×10^{-6}	9.0166×10^{-7}
n	7.2751×10^{-1}	7.8734×10^{-1}	7.5627×10^{-1}
c	3.8049×10^{4}	1.0039×10^{5}	1.0643×10^{5}
d	4.384×10^{0}	1.617×10^{1}	1.5652×10^{1}
h	-5.7058×10^{-1}	-5.9825×10^{-1}	-4.3884×10^{-1}
$r(\AA)$	1.8	2.7	2.8
$S(\AA)$	2.1	3.0	3.1

$\chi_{SiC} = 0.9776 \qquad \chi_{siGe} = 1.00061$

Chapter 3

Crystal Properties

a.) Static Structural Properties

The static structural properties such as lattice constant, cohesion energy, bulk modulus and elastic constants can be obtained from the calculated total energy as a function of volume for the observed crystal structure.

Any undistorted crystal structure can be defined as an arrangement of N cells, each containing n atoms, by

$$\mathbf{R}_l^k = \mathbf{R}_l + \mathbf{d}^k \tag{3.1}$$

where k runs from 1 to n and $\mathbf{R}_l^k$ expresses the vector position of each atom in the solid in terms of the primitive real-space Bravais lattice vectr $\mathbf{R}_l$ specifying its cell, and the vector position $\mathbf{d}^k$ of the atoms inside the cell. These two vectors, expressed on the basis vector $\mathbf{a}_i$, are

$$\mathbf{R}_l = l_1\mathbf{a}_1 + l_2\mathbf{a}_2 + l_3\mathbf{a}_3 \tag{3.2.a}$$

$$\mathbf{d}^k = x_1\mathbf{a}_1 + x_2\mathbf{a}_2 + x_3\mathbf{a}_3 \tag{3.2.b}$$

where $0 \leq x_i < 1$.

It is experimentally known that the most stable structure of semiconductors at conditions of low temperature and pressures is the diamond structure (when

mixed is called zinc–blende). To calculate the equilibrium lattice parameter and the cohesion energy for this structure it is necessary to evaluate the energy at different values of vectors positions $\mathbf{R}_l^k$ in order to find the configuration with minimum energy. At this value the energy is called the cohesion energy and its correspondent distance in the Bravais lattice is the equilibrium lattice parameter.

The bulk modulus is given by:

$$B = -\Omega \left(\frac{\partial P}{\partial \Omega}\right)_T = \Omega \left(\frac{\partial^2 E}{\partial \Omega^2}\right)_T \tag{3.3}$$

but we can write the second derivative as

$$\frac{\partial^2 E}{\partial \Omega^2} \simeq \frac{2 \triangle E(\Omega)}{\Omega^2} \tag{3.4}$$

where $\triangle E(\Omega) = E(\Omega) - E(\Omega_o)$ and this value is easy to calculate directly from the energy as function of the volume Ω.

From the theory of elasticity[30], we know that a macroscopic vector $\mathbf{R}$ joining two points in a unstressed solid is carried under stress to a nearby vector $\mathbf{R}'$ so that

$$\mathbf{R} - \mathbf{R}' = \Phi \cdot \mathbf{R} \tag{3.5}$$

where by definition Φ is the (constant) strain tensor, if the deformation is homogeneous. By writing

$$\mathbf{R} = l_1 \mathbf{a}_1 + l_2 \mathbf{a}_2 + l_3 \mathbf{a}_3 \tag{3.6.a}$$

$$\mathbf{R}' = l_1 \mathbf{a}'_1 + l_2 \mathbf{a}'_2 + l_3 \mathbf{a}'_3 \tag{3.6.b}$$

where l_i are integers and $\mathbf{a}'_i$ are the primitive translation vectors in the strain solid and substituting $\mathbf{R}$ and $\mathbf{R}'$ in the equation (3.5), this takes the following form:

$$\mathbf{a}_i - \mathbf{a}'_i = \Phi \cdot \mathbf{a}_i \qquad\qquad i = 1, ..., 3 \tag{3.7}$$

This equation means that the unit cell undergoes exactly the same (fractional) deformation as does the whole crystal. Translational invariance, which defines the crystalline state, requires a homogeneous deformation to be retained down to the smallest lattice vector.

The elastic constants are defined with respect to a cartesian coordinate system oriented in some conventional way with respect to the crystal axes. Hence equation (3.7), although independent from the coordinate system, enables the calculation of the axes (in length and direction) of the deformed crystal from those of the undeformed crystal and from the usual cartesian strain tensor

$$e = e_1, e_2, ..., e_6$$

where the indexes are conventionally defined, to simplify the notation, by

$$xx \rightarrow 1, yy \rightarrow 2, zz \rightarrow 3, yz \rightarrow 4, zx \rightarrow 5, xy \rightarrow 6.$$

The increase δE in energy per unit cell is related to the elastic constants C_{ij} (at 0^oK) via the general equation

$$\frac{\delta E}{\Omega} = \frac{1}{2} \sum_{ij}^{6} C_{ij} e_i e_j \tag{3.8}$$

where Ω is the unit cell volume. These are as many linearly independent equations as there are elastic moduli, and they constitute a set of conditions on the parameters of the potential energy function.

It is also required that the unstrained crystal shall be in equilibrium under any assumed potential function at the observed crystal structure. Formally this is

$$\left(\frac{\partial E}{\partial e}\right)_o = 0 \tag{3.9}$$

where e denotes any strain and the derivatives are to be evaluated in the state of zero strain. The elements of the strain tensor are of the form $(\partial v_i/\partial x_j)$, where the v_i are the components of the displacements and the x_j are cartesian coordinates.

Knowing the potential–energy function for a specific crystal, its elastic constants are easily computed[31]. By suitably choosing the nonvanishing strains, only a few (in some case just one) of the C_{ij}, remain the right–hand side of equation (3.8). For such choice, at a number of equally spaced small strains, the deformed a_i' are computed from equation (3.7) knowing the lattice parameter of this structure. If the second differences of the potential energies are constant, then the strains are within the Hooke's law range and the combination of elastic constants is simply proportional to the second difference. Moreover the necessity that strains equivalent in symmetry should present identical potential energies, permits to perform additional checks with the purpose of obtaining a more preciser computation.

With this method it is possible to determine every elastic constant. For instance, if we choose $e_1 = e$ and all the other values of the strain tensor equal to zero, it is possible to establish C_{11}. If we choose $e_4 = e$ and the others equal to zero, we can calculate C_{44}, and for $e_1 = e$ and $e_2 = e$, it is possible to determine $C_{11} + C_{12}$. This set of equation gives us the possibility of calculating all the elastic constants for a cubic crystal.

In our case to compute the elastic constants of semiconductors, a strain region from 0 to 0.04 $\mathring{A}$ was chosen, where the relation is kept linear according to the law of Hooke.

The results for these elements are given in table I, where we compare the results predicted by the Tersoff potential with experimental measurements. The agreement is particularly good in the case of simple elements. For mixtures such as SiC the concordance is good for cohesion energy, lattice parameter and bulk

modulus but rather poor for the elastic constant C_{44}, whose value is almost twice the experimental one.

TAB. 2.1: Comparison of calculated lattice constants a($\AA$), cohesive energies E_{coh}(eV) per atom, bulk moduli B(Mbar) and elastic constants (Mbar) of C, Si, Ge, SiC and SiGe with experimental data given in parenthesis.

	C	Si	Ge	SiC	SiGe
a	3.56 (3.56)	5.43 (5.43)	5.65 (5.65)	4.32 (4.36)	5.54 (5.57)
E_{coh}	7.37 (7.37)	4.63 (4.63)	3.85 (3.85)	6.18 (6.34)	4.23 (4.35)
B	4.55 (4.00)	0.78 (0.99)	0.55 (0.77)	2.24 (2.2)	1.33
C_{11}	10.9(10.8)	1.3 (1.7)	1.2 (1.3)	4.2 (3.6)	1.8
C_{12}	1.22 (1.3)	0.52 (0.6)	0.21 (0.48)	1.2 (1.5)	1.1
C_{44}	6.4(5.8)	0.99 (0.8)	0.82 (0.67)	2.6 (1.5)	1.02

b.) Crystal Stability

The presence of an absolute minimum of the total free energy in a certain configuration constitutes both a necessary and a sufficient condition for the stability of this configuration in the dynamical sense. However, other local minima of the free energy surface could also exist, corresponding to different, metastable structures. The difference in free energy between the various structures depends in general upon thermodynamical variables such as temperature and pressure. Therefore, phase transitions between different structures can be induced by changes in the thermodynamical condictions. For instance in semiconductors the diamond structure is known to be the most stable at low temperature and pressure. However, for example, silicon at a pressure of $\sim$ 125 Kbar transforms to the metallic body-centered tetragonal β–tin structure[32], and for germanium the β–tin phase has also been observed at pressures of $\sim$ 100 Kbar[33].

While studing the effect of temperature requires a full treatment of the free energy, which often requires a major effort to be carried out, the effect of pressure at $T = 0$ can be investigated by simple static calculations.

TAB. 2.2: Packing fraction (c/a) for the β–tin structure, the packing fraction for C was chose as the value of the tin at room temperature. The packing fractions of Si and Ge are chosen from experimental data.

	Packing fraction
C	0.5462
Si	0.5516
Ge	0.5512

In order to compare the different structures we have carried out calculations on the diamond, β–tin, bcc, fcc and simple cubic(sc) structures for Si, Ge, C, and on the zinc blende and rocksalt structures for SiC and SiGe. The packing fraction is given in the table 2.2 for the β-tin structure.

To compare our calculation with results from density functional theory in the local density approximation, we calculated the energy of each phase at its minimum energy lattice spacing, relative to that of the diamond phase:

$$\Delta E = E_{min}^{phase} - E_{min}^{diamond} \tag{3.10}$$

The results are given in tables 2.3 and 2.4, and show that, as expected, the diamond(or zinc–blende) structure is the most favoured at zero pressure.

TAB. 2.3: Relative energy ΔE of various crystal phases at their minimum in energy for carbon, silicon and germanium. The values in parenthesis are the density functional theory results.

	C	Si	Ge
diamond	0.00 (0.00)	0.00 (0.00)	0.00 (0.00)
$\beta - tin$	2.91 (2.82)	0.36 (0.27)	0.35 (0.25)
Simple Cubic	2.90 (2.66)	0.32 (1.1)	0.33 (0.31)
fcc	4.34 (4.59)	0.76 (1.25)	0.53 (0.46)
bcc	3.69 (4.28)	0.43 (1.12)	0.35 (0.44)

In figures 3.1–3.3 we present the energy as a function of the atomic volume

TAB. 2.4: Relative energy ΔE of various crystal phases at their minimum in energy for SiC and SiGe (the stable stucture is zinc blende).

	SiC	SiGe
zinc blend	0.00	0.00
rocksalt	2.36	0.25
fcc	1.29	0.83
bcc	2.49	0.39

also the Enthalpy $H = E + P\Omega$ as a function of Pressure (P) for these phases for C, Si, Ge . From these figures and the results of table 2.3, we can observe that this potential does not predict a pressure–induced transition from the diamond to the β–tin structure, only predicts a transition to a bcc structure for Si and Ge at high pressure. For C the diamond structure is always the most stable structure. Furthermore, these calculations show that the simple metallic phases of C have small cohesive energies and relatively large equilibrium volumes as compared with diamond, in agreement with experimental studies.

For SiC, in metallic structures like the rocksalt (rs) one there is a good agreement with the theoretical calculations performed using LDA by Chang and Cohen[34], with respect at lattice parameter. For[35] SiGe this potential predict a transition from the zinc blende to the bcc(si–ge) structure.

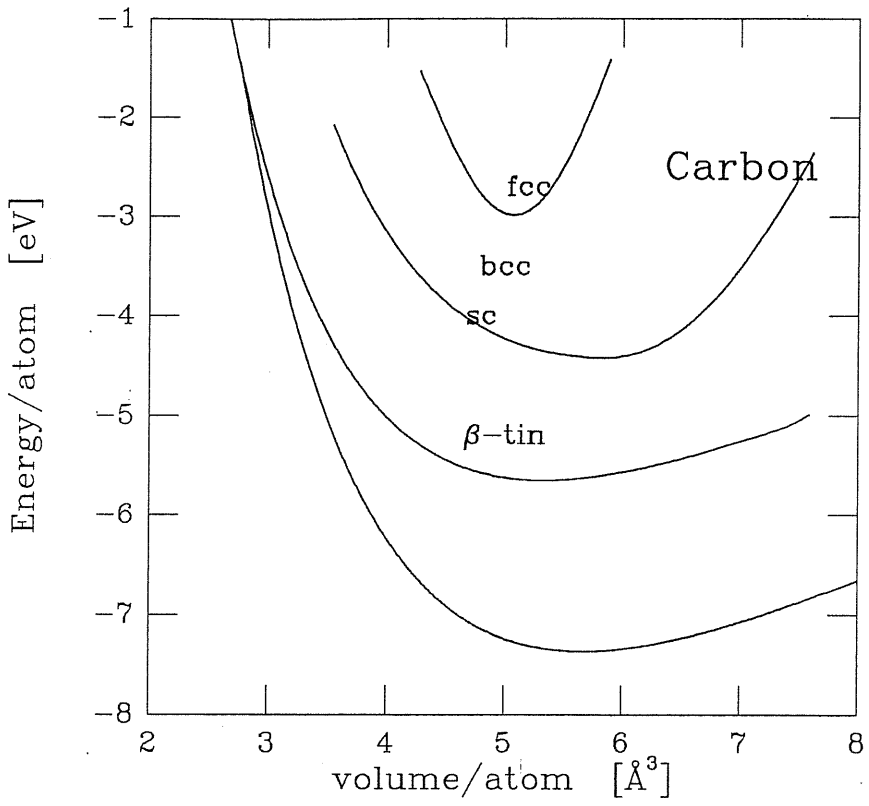

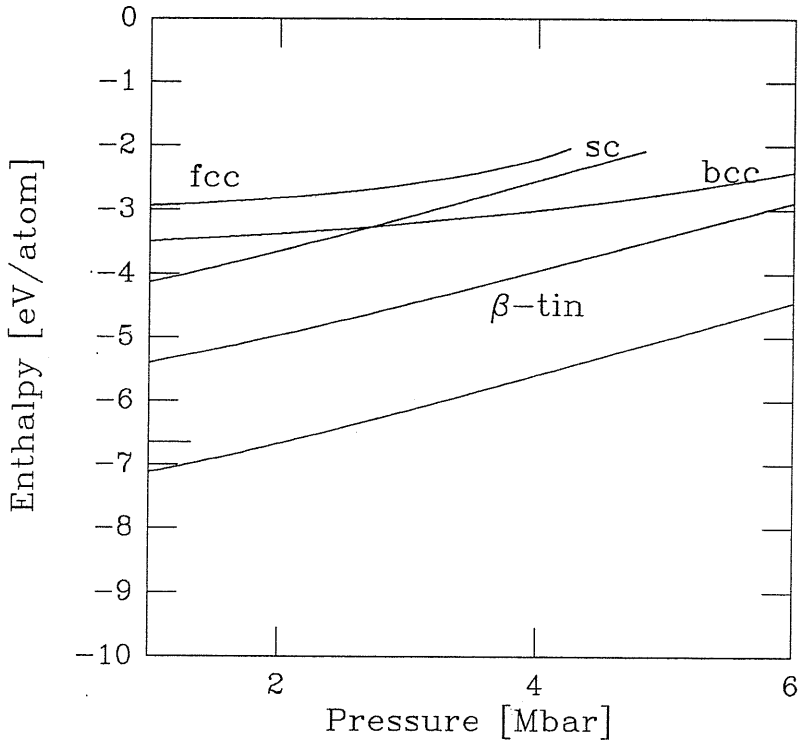

FIG. 3.1: Energy per atom in function of atomic volumen for various crystal phases calculated using the Tersoff potential and its corresponding Enthalpy as a function of Pressure for carbon.

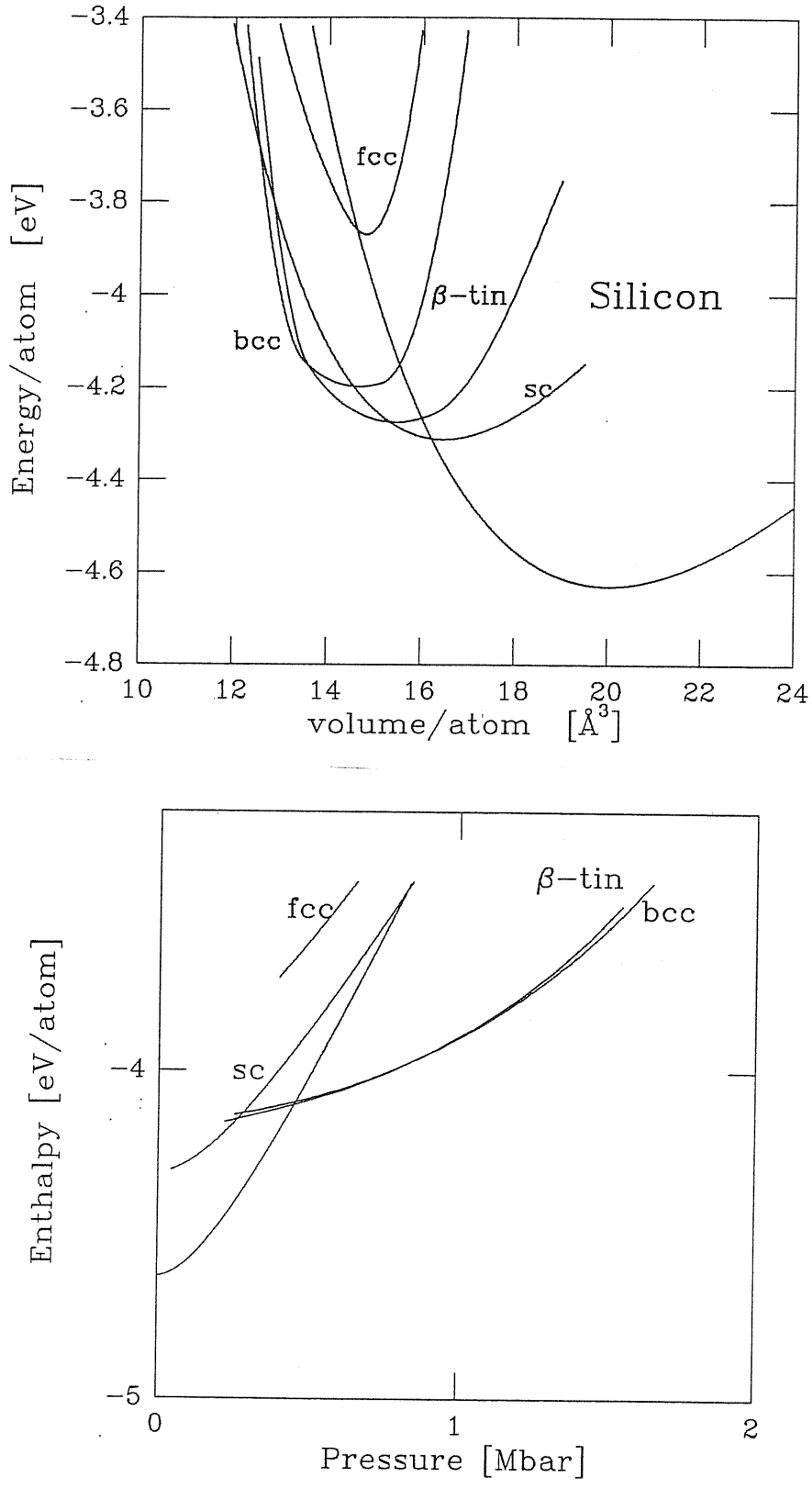

FIG. 3.2: Energy per atom in function of atomic volumen for various crystal phases calculated using the Tersoff potential and its corresponding Enthalpy as a function of Pressure for Silicon.

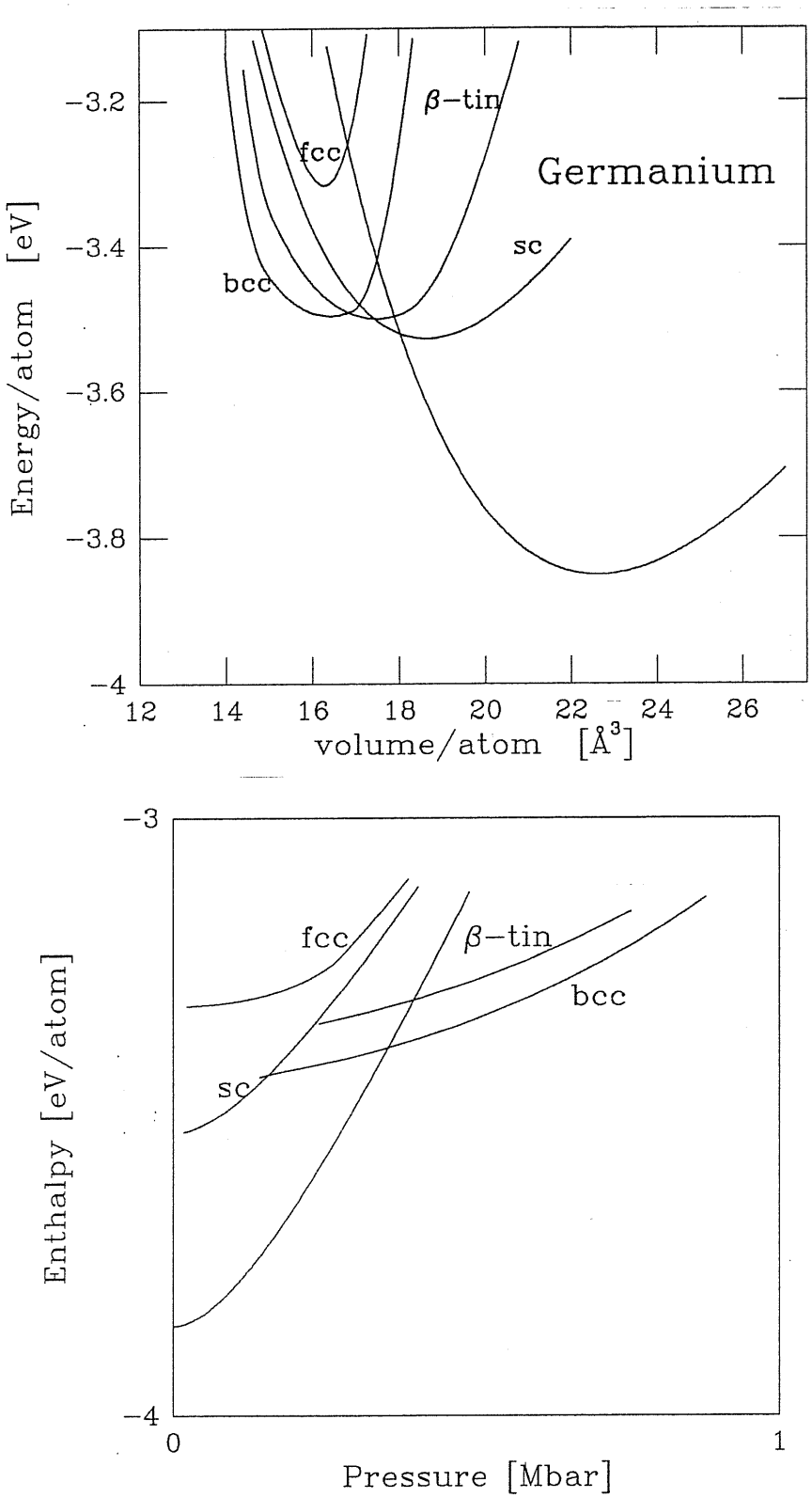

FIG. 3.3: Energy per atom in function of atomic volumen for various crystal phases calculated using the Tersoff potential and its corresponding Enthalpy as a function of Pressure for Germanium.

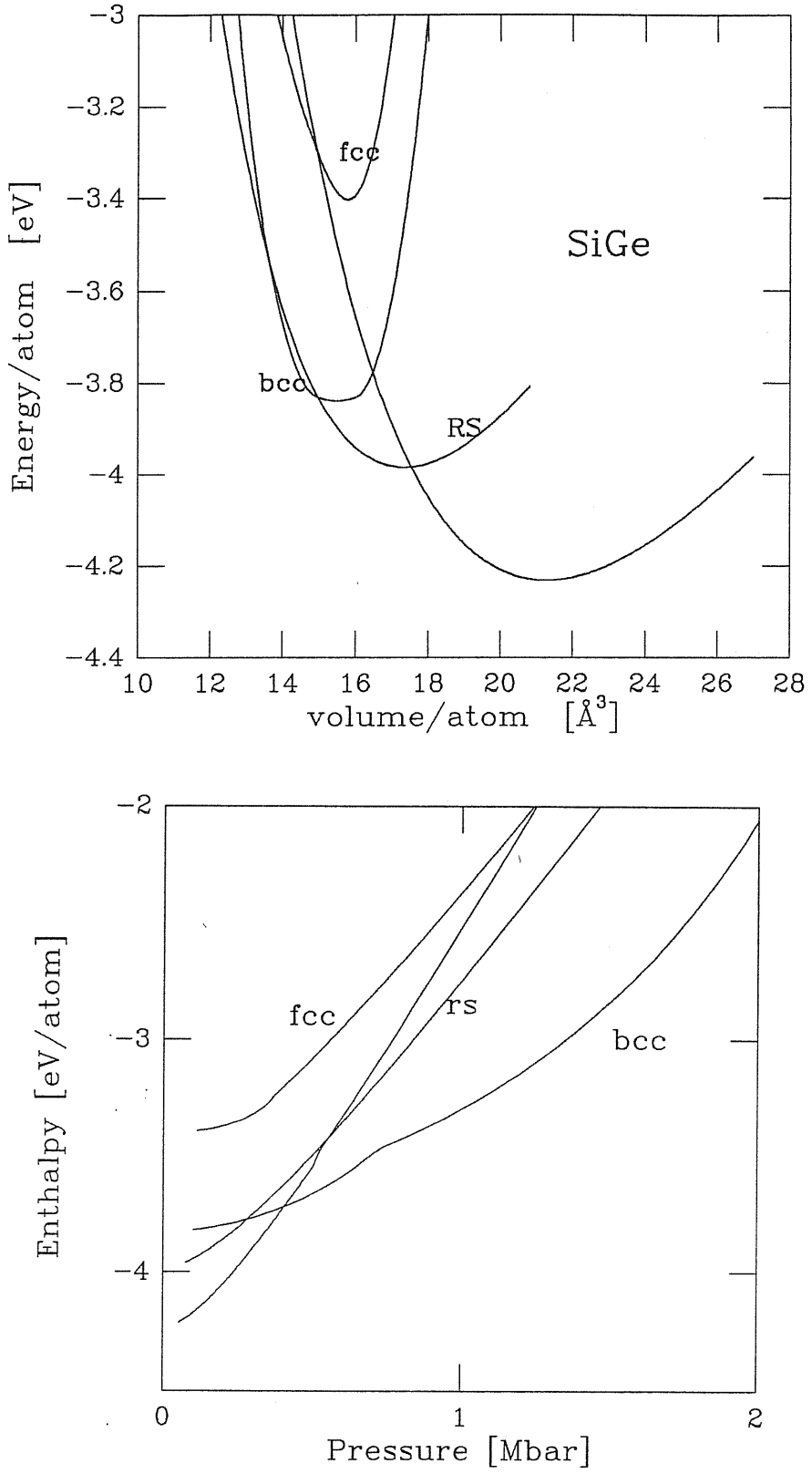

FIG. 3.4: Energy per atom in function of atomic volumen for various crystal phases calculated using the Tersoff potential and its corresponding Enthalpy as a function of Pressure for SiGe.

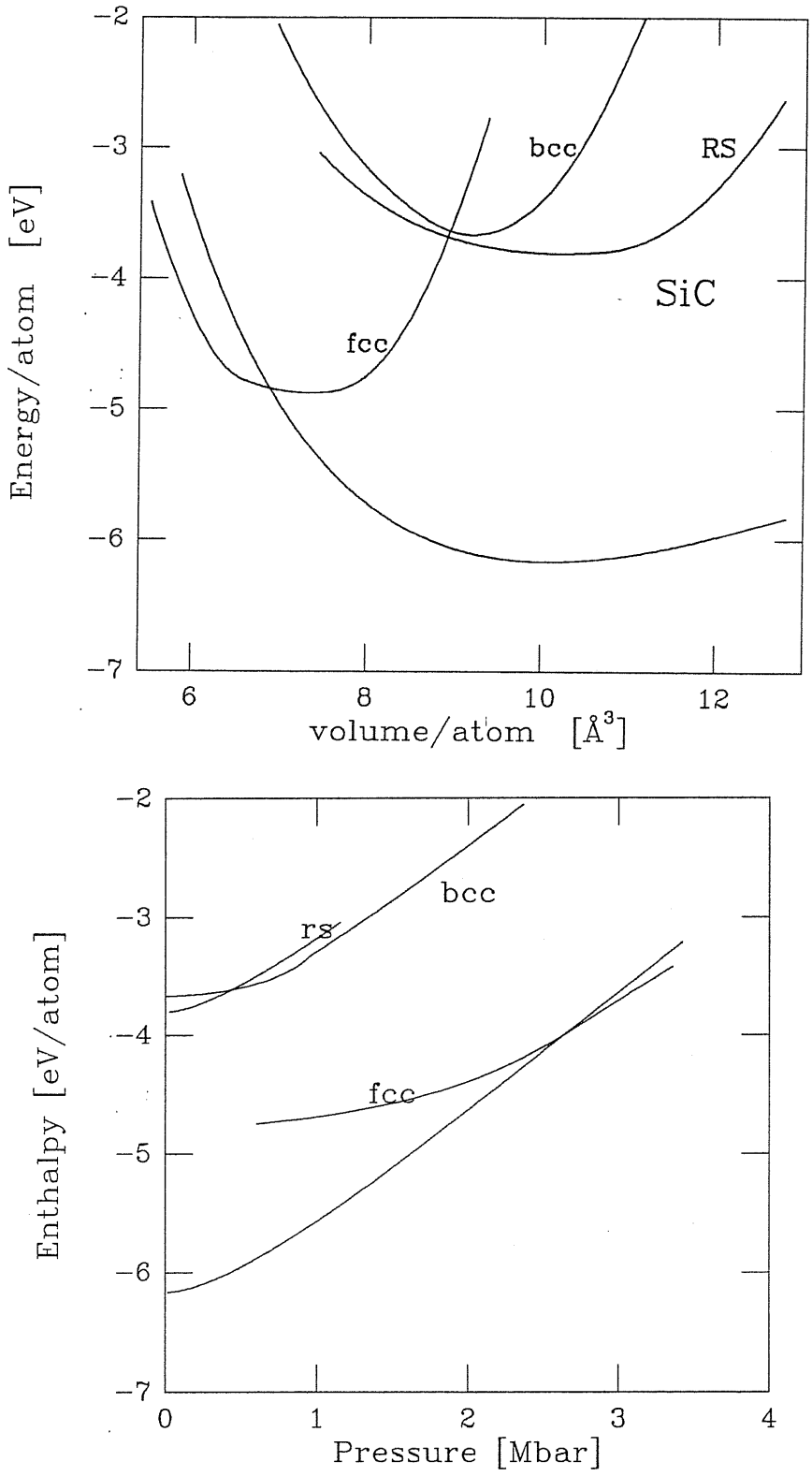

FIG. 3.5: Energy per atom in function of atomic volumen for various crystal phases calculated using the Tersoff potential and its corresponding Enthalpy as a function of Pressure for SiC.

c.) Phonon Energy and Phonon Density of States

Let us consider a small displacement $\mathbf{U}_l^k$ of the atoms in the crystal defined in the following way

$$\mathbf{R}_l^k = \mathbf{R}_l + \mathbf{d}^k + \mathbf{U}_l^k \tag{3.11}$$

The theory of the lattice dynamics in the harmonic and adiabatic approximation is formulated in terms of the dynamical matrix[30,36], which in direct space is given by:

$$D_{\alpha\beta}^{kk'} = \left(m^k m^{k'}\right)^{\frac{1}{2}} \varphi_{\alpha\beta}^{kk'}\left(\mathbf{R}_l - \mathbf{R}_{l'}\right) \tag{3.12}$$

where m_k is the mass of the k-th atom in the unit cell and

$$\varphi_{\alpha\beta}^{kk'} = \left(\frac{\partial^2 E}{\partial U_{l\alpha}^k \partial U_{l'\beta}^{k'}}\right)_0 \tag{3.13}$$

are the force constants, and E is the total energy, α and β are the cartesian directions and $(...)_0$ indicates that the derivative has to be evaluated with the atoms in their perfect crystal positions.

Phonon frequencies and polarizations can be calculated directly from the eigenvalues and eigenvectors of the dynamical matrix in reciprocal space

$$D_{\alpha\beta}^{kk'}(\mathbf{q}) = \sum_{\mathbf{R}_l} D_{\alpha\beta}^{kk'}(\mathbf{R}_l)\exp^{-i\mathbf{q}\cdot(\mathbf{R}_l+\mathbf{d}^k-\mathbf{d}^{k'})} \tag{3.14}$$

through the eigenvalue equation

$$\omega^2(\mathbf{q})e_\alpha^k(\mathbf{q}) = \sum_{k'\beta} D_{\alpha\beta}^{kk'}(\mathbf{q})e_\beta^{k'}(\mathbf{q}) \tag{3.15}$$

Solving this equation we obtain ω^2, where $\omega = 2\pi\nu$ and ν is the phonon frequency.

For example, in the special case of the diamond structure there are two atoms per unit cell and therefore we have to diagonalize a 6×6 matrix.

The analytical evaluation of the second derivatives of the Tersoff potential is very complicated. For this reason we have calculated them by numerical differentiation of the first derivative of the energy, e.g. as the first derivative of the force

$$F_{l\alpha}^{k} = -\frac{\partial E}{\partial U_{l\alpha}^{k}} \tag{3.16}$$

An important quantity is the frequency distribution function or frequency spectrum $g(w)$ of vibrations, which gives the number $g(w)dw$ of vibrations with frequencies between w and $w+dw$. This number is, of course, different for different branches of the spectrum.

$g(\omega)d\omega$ is given by the $\mathbf{q}$ space volume divided by $(2\pi)^3$ that lies between two infinitesimally close surfaces of constant frequency $\omega(\mathbf{q}) = \text{const}$. The distance between two such surfaces (measured along the segment of the normal between them) is $\frac{dw}{|\nabla_q w|}$ and multiplying this term by the area dS of the constant-frequencies surface element and integrating over the whole surface, one obtains the well–know formula

$$g(\omega) = \frac{\Omega}{(2\pi)^3} \sum_j \int_{\omega(\mathbf{q})=\omega} \frac{dS}{\mid \nabla_q \omega_j(\mathbf{q}) \mid} \tag{3.16}$$

where the integral is taken over the surface of constant frequency ω, and j are the branches of the spectrum.

In order to calculate this expression, Jepsen and Andersen[37] propose the so–called "tetrahedron method", where one divides the irreducible wedge of the Brillouin zone into tetrahedra and the integral (2) is then evaluated as the sum

$$g(w) = \frac{\Omega}{(2\pi)^3} \sum_{ji} g_{ji}(w) \tag{3.17}$$

where $g_{ji}(w)$ is the partial number of states and also the volume of that part of the i-th tetrahedron in which $w_j(k)$ is less than w.

Applying this method[38] in the irreducible wedge of the Brillouin zone and evaluating the frequency in 80 points, we obtain the phonon density of states.

In order to calculate the frequencies, it is necessary to find the regime where the force as a function of the displacement is linear in any direction. We have found that this occurs when the displacement is between 0.0 and 0.04$\mathring{A}$. For our calculation we have chosen a displacement of 0.02$\mathring{A}$. With the aim of limiting errors due to the presence of anharmonic terms, we took into account the displacements in both the negative and positive sense obtaining a greater accuracy. In the figures 3.4– 3.8 we present the dispersion curves and bulk DOS predicted by the Tersoff potential for the elements and compounds studied. Some numerical values at high-symmetry points Γ, X and L are also reported in table 2.5 in comparison with experimental data.

For simple semiconductors, we observe from the dispersion curves and table 2.5 that the width of the spectrum is slightly larger than that obtained experimentally. The transverse acustic mode frequencies are overestimated. In the optical mode and near the zone boudary the frequencies of the phonon spectrum are overestimated with respect to the experimental values. On the other hand, there is good agreement in the acustic mode, which simply reflects the fact that the potential is fitted to the elastic constants.

TAB. 2.5: Phonon frequencies $[cm^{-1}]$ calculated at the high-symmetry points Γ, X and L for five components. Experimental data are in parenthesis.

	C^a	Si^b	Ge^c	SiC	SiGe
Γ_{TO}	1570 (1326)	536 (517)	330 (304)	949	423
Γ_{LO}	1570 (1326)	536 (517)	330 (304)	949	423
X_{TA}	1006 (797)	230 (150)	156 (80)	523	192
X_{LA}	1255 (1071)	407 (410)	253 (241)	715	318
X_{TO}	1301 (1194)	497 (463)	282 (276)	797	327
X_{LO}	1301 (1194)	497 (410)	282 (241)	821	375
L_{TA}	704 (636)	156 (114)	111 (63)	362	134
L_{LA}	1138 (1069)	377 (378)	245 (222)	713	306
L_{TO}	1418 (1234)	514 (487)	307 (290)	884	399
L_{LO}	1402 (1277)	439 (417)	246 (245)	788	329

a experimental data from Ref.[39]

b experimental data from Ref.[40]

c experimental data from Ref.[41]

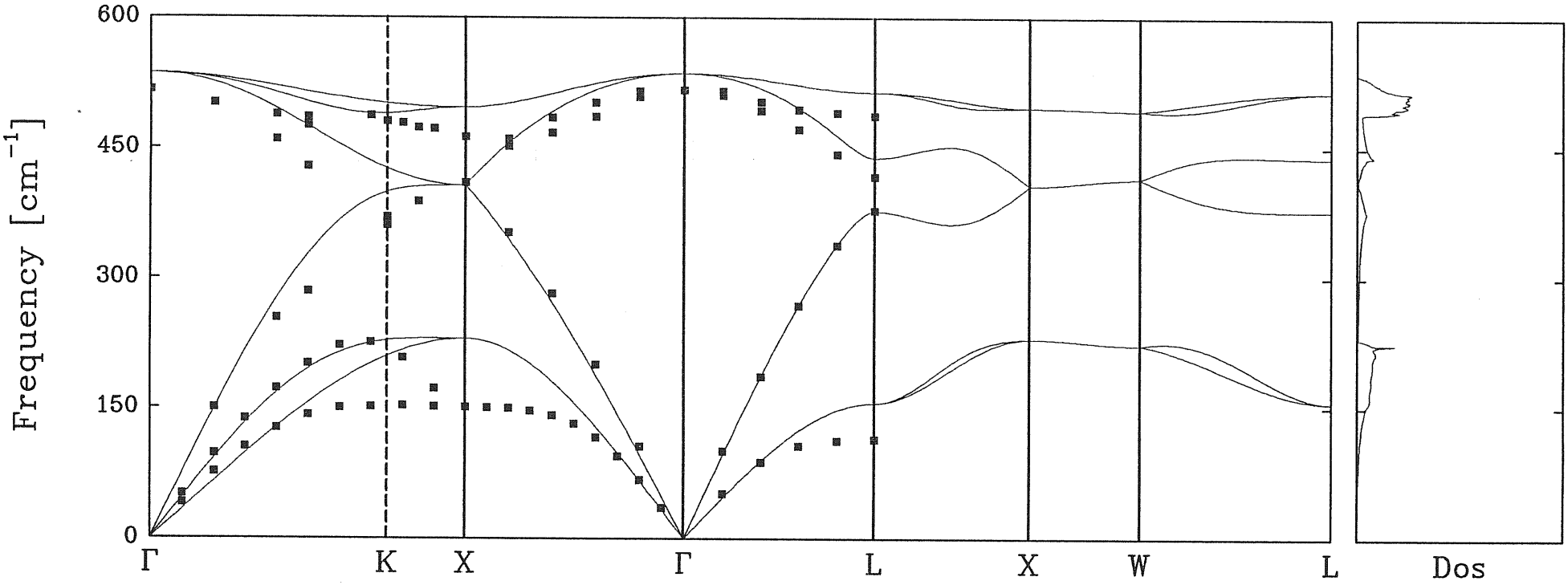

FIG. 3.5: Bulk–Si phonon dispersion curves from the Tersoff potential compared with experimental. Also the bulk phonon density of states.

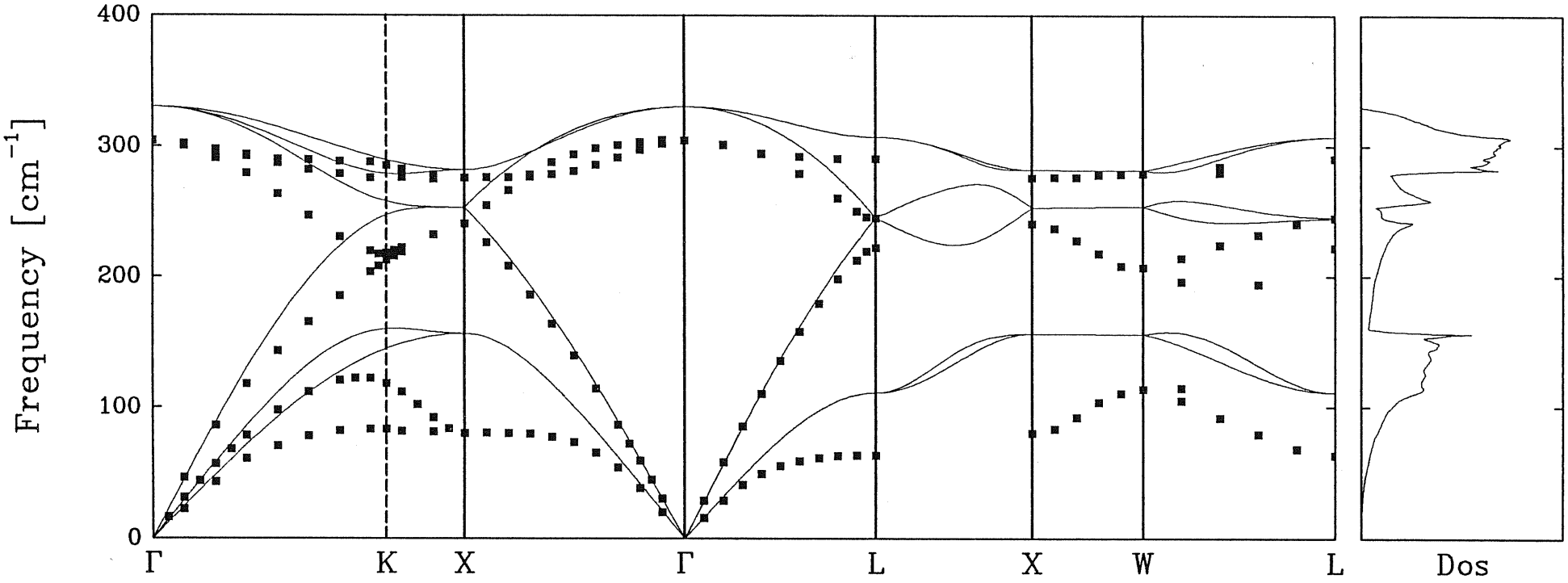

FIG. 3.5: Bulk–Ge phonon dispersion curves from the Tersoff potential compared with experimental. Also the bulk phonon density of states.

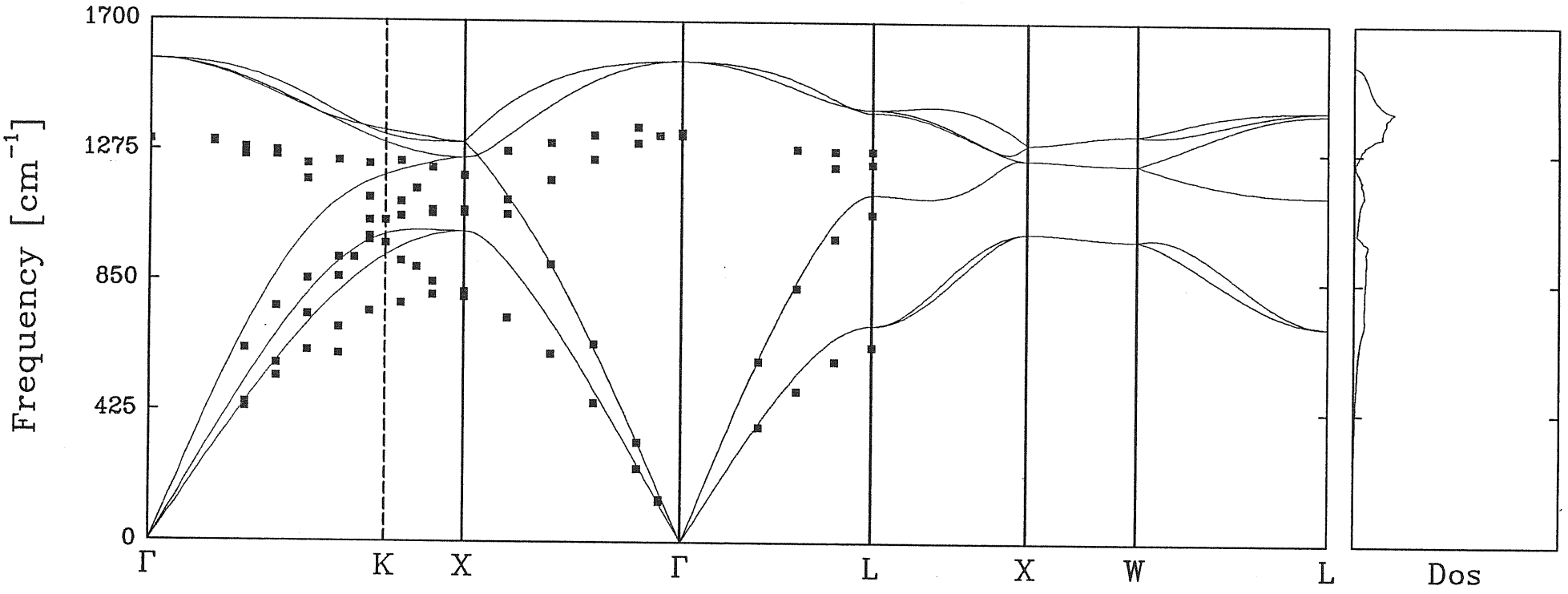

FIG. 3.4: Bulk–C phonon dispersion curves from the Tersoff potential compared with experimental. Also the bulk phonon density of states for these elements.

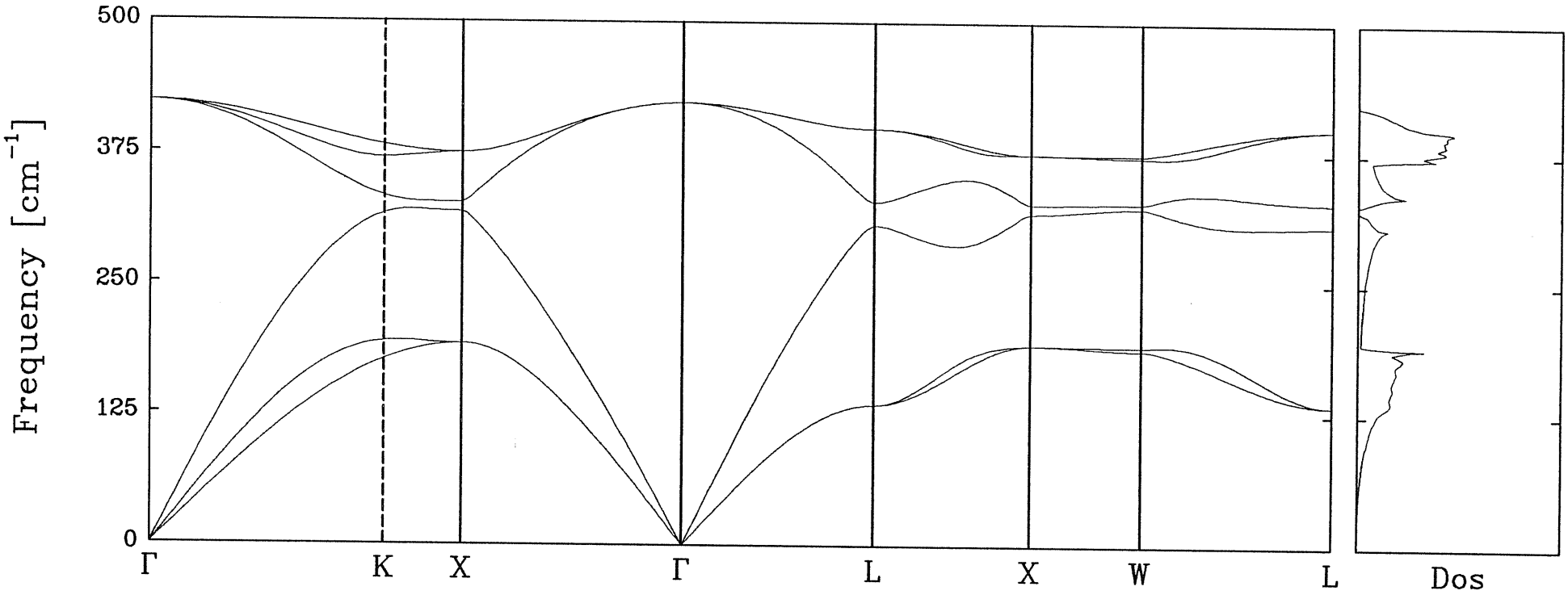

FIG. 3.5: Bulk–SiGe phonon dispersion curves from the Tersoff potential. Also the bulk phonon density of states.

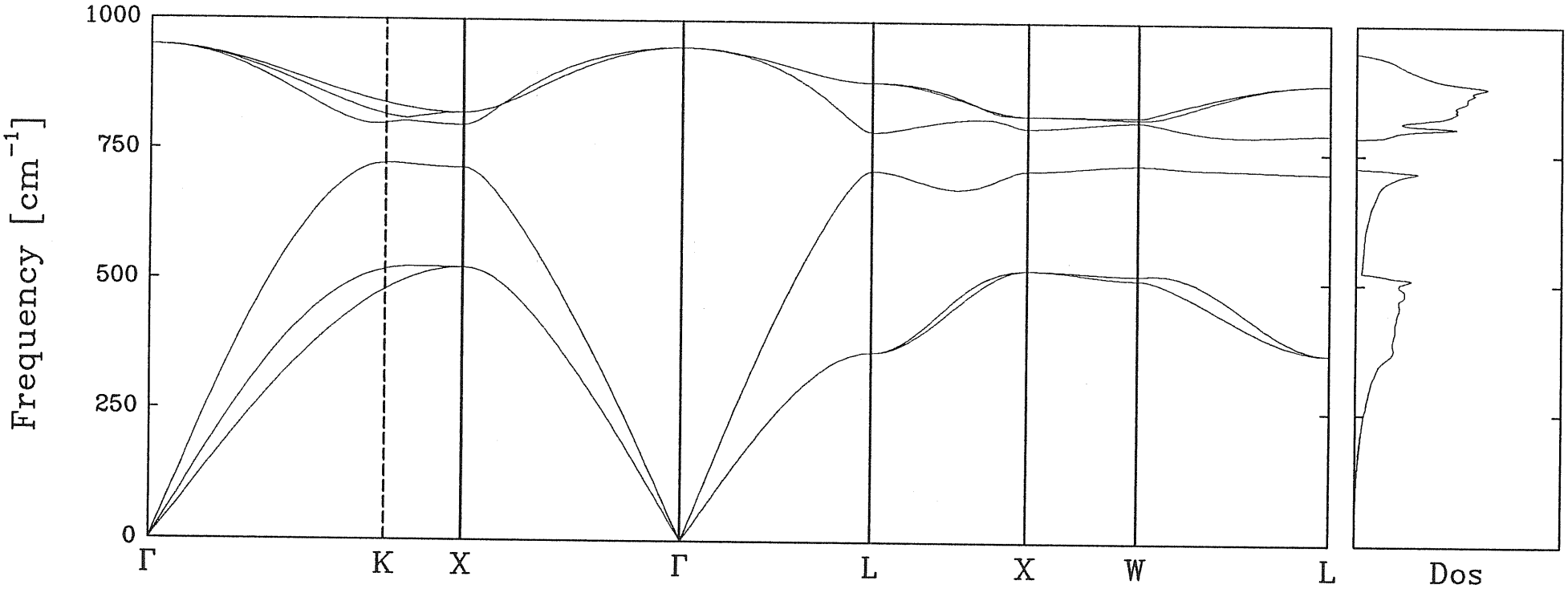

FIG. 3.5: Bulk–SiC phonon dispersion curves from the Tersoff potential. Also the bulk phonon density of states.

Chapter 4

Point Defects

In order to study the energetics of point defects this chapter and surface reconstructions (chapter 4), it is necessary to find the minimum energy of a system with low symmetry and many degrees of freedom. Several relaxation techniques could be used to this purpose.

In this thesis, we have made extensive use of molecular dynamics, which is a well–known method to obtain the motion of a given number of atoms governed by their mutual interatomic interactions by numerical integration of the Newton's equations of motion

$$\mathbf{F}_i = -\frac{\partial E}{\partial \mathbf{R}_i} \tag{4.1}$$

where i is the particular index.

In our case, we have used $\mathbf{F}_i$ as resulting from using the Tersoff potential (see Appendix 1). The computer code uses a fifth–order predector–corrector algoritmo[42], and Verlet neighbour–lists constructed by a variant of the cell method[43]. The time step (Δt) used was ($0.002ps$) for silicon, which is a small fraction of the silicon-optical phonon period ($0.0638ps$). A similar (Δt) has been chosen for the other materials studied.

This type of approach is naturally aimed at studying finite temperature properties, but it can also be effectively used as an energy minimization tool. This is obtained by gradually removing kinetic energy from the system, until the particles have come to an equilibrium position. Two methods were used to this purpose:

1.) " quenching ", which consists in driving the system, by a direct cooling

towards the nearest (or one of the nearest) energy local minimum. To this purpose, all the velocities are scaled by a factor $\alpha < 1$ at each time step of the simulation.

2.) "simulated annealing" which consists of thermally annealing the system at finite temperature and then cooling it gradually down to T=0.

We want to make a general consideration about these two methods and about their positive or negative aspects. The quenching procedure is faster, however the danger of remaining trapped in a local energy minimum is very high. On the other hand, the computer time required for simulated annealing is much longer, but energy barriers can be eliminated and the real energy minimum can be reached, if it is deep enough and in spite of the fact that the initial conditions were very far from this minimum. Therefore, the use of simulated annealing for energy minimization presents a clear advantage over traditional methods in "complex" optimization problems, that is when several local minima are present and an exhaustive search is too expensive to perform.

a.) Point Defects

One interesting and technologically important problem in condensed matter physics is understanding point defects, particularly in semiconductors. In determining the mechanism and rate of diffusion in solids, formation and migration energies of point defects are extremely important quantities that are widely studied experimentally and theoretically.

We want here to investigate the Tersoff potential's ability to model defects in the diamond lattice. We recall that atoms located in noncrystallographic atomic positions in the crystal of a determined element are called self–interstitials, and the lack of one atom in this type of structure is called vacancy.

We have investigated two different types of self–interstitials. Tetrahedral site (T) and hexagonal site (H) interstitials are located respectively at $(a/2, a/2, a/2)$ and $(5a/8, 5a/8, 5a/8)$ in the diamond unit cell, where a is the lattice parameter of the crystal. We have also studied the vacancy and the split–vacancy. All these points defects are represented in the below figure

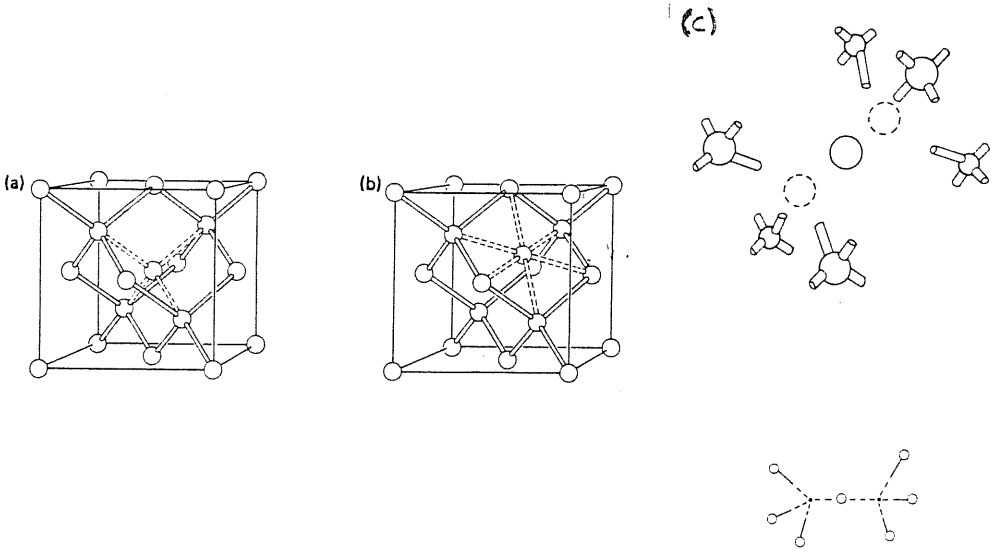

FIG. 4.1: Representation of the point defects in the unit cell. (a) Tetrahedral site interstitial, (b) Hexagonal site interstitial and (c) split vacancy.

The vacancy formation energy (E_f^V) in a N–atoms cell is defined as:

$$E_f^V = E^V - \frac{N-1}{N} E_{bulk} \tag{4.2}$$

where E^V is the total energy per supercell containing the vacancy and E_{bulk} is the total energy per supercell of a perfect crystal. Analogously the formation energy of an interstitial, (E_f^I) is given by:

$$E_f^I = E^I - \frac{N+1}{N} E_{bulk} \tag{4.3}$$

where E^I is the total energy per supercell containing an interstitial point defect.

These formation energies provide a direct information on the concentration of defects as a function of temperature (i.e.,$\sim exp(-E_f/K_BT)$). However, they cannot say anything about the migration rate of defects, which is the other crucial ingredient determining the diffusion coefficient. In fact, migration is controlled by energy barriers that the defect has to cross in order to jump from a lattice site to an adjacent one, or to some intermediate metastable configuration. In the vacancy case, we have made a study of the height and shape of this barrier, reported in the next section.

b.) Computational Method

While the determination of $T = 0$ formation energies is relatively straightforward–being sufficient to relax the system using one of the procedures outlined in the previous section–studying the shape of the energy barrier to migration is slightly more complicate. In fact, relaxation should always be allowed to occur to study realistically the potential energy surface. However, the system is stable only when the jumping atom is in a lattice site (and the vacancy in another), or halfway between two lattice sites (split vacancy). For all other positions, a constraint has to be imposed to prevent the atom from falling back in the equilibrium position during the relaxation. This is done by keeping fixed the "reaction coordinate" (ξ),

defined as[44]

$$\xi = \frac{1}{6}\sum_{i=1}^{6}(\mathbf{R}_i - \mathbf{R}_o)\cdot\mathbf{J} \tag{4.4}$$

where $\mathbf{R}_o$ is the coordinate of the jumping atom, and $\mathbf{R}_i$ those of the neighboring atoms. $\mathbf{J}$ is a unit vector indicating the direction of the jump. The number 6 appears because there are 6 neighbours around the vacancy. ξ takes values from $-d/2$ to $d/2$, where d represents the bond length. Two characteristic points are $\xi = 0$, which corresponds to the split vacancy, and $\xi = \pm 0.5$ corresponding to the simple vacancy.

For interstitial point defects both hexagonal and tetrahedral all the coordinates close to the interstitial are considered. For the hexagonal side they are at the number of 6, while for tetrahedral one they are 4. We have found the position of interstitial atom at every step taking into consideration its neighboring atoms and positioning the interstitial atom in its ideal interstitial position.

In our simulation we considered a system containg 215 atoms for the vacancy case and 217 for the interstitial case, using periodic boundary conditions. We have tested that ths number of atoms is large enough to keep small size effects arising from the interaction of the defect with its images in the neighbouring supercells. In all the cases, the starting point was a configuration where the atoms occupy lattice sites and the velocities are zero. When the simmulation has started, atoms begin to move towards the equilibrium positions, and they gain a kinetic energy. At each time step, part of the kinetic energy is removed by velocity scaling, driving the system towards the energy minimum. When the kinetic energy becomes neglectable, the defect energy is obtained by (4.1) or (4.2). In figure 4.2, we show the kinetic and potential energy as a function of time for Germanium in the point at $\xi = 0$ (split vacancy) and a velocity scaling factor $\alpha = 0.95$. The

system reaches an almost complete rest state after about 300 MD time steps.

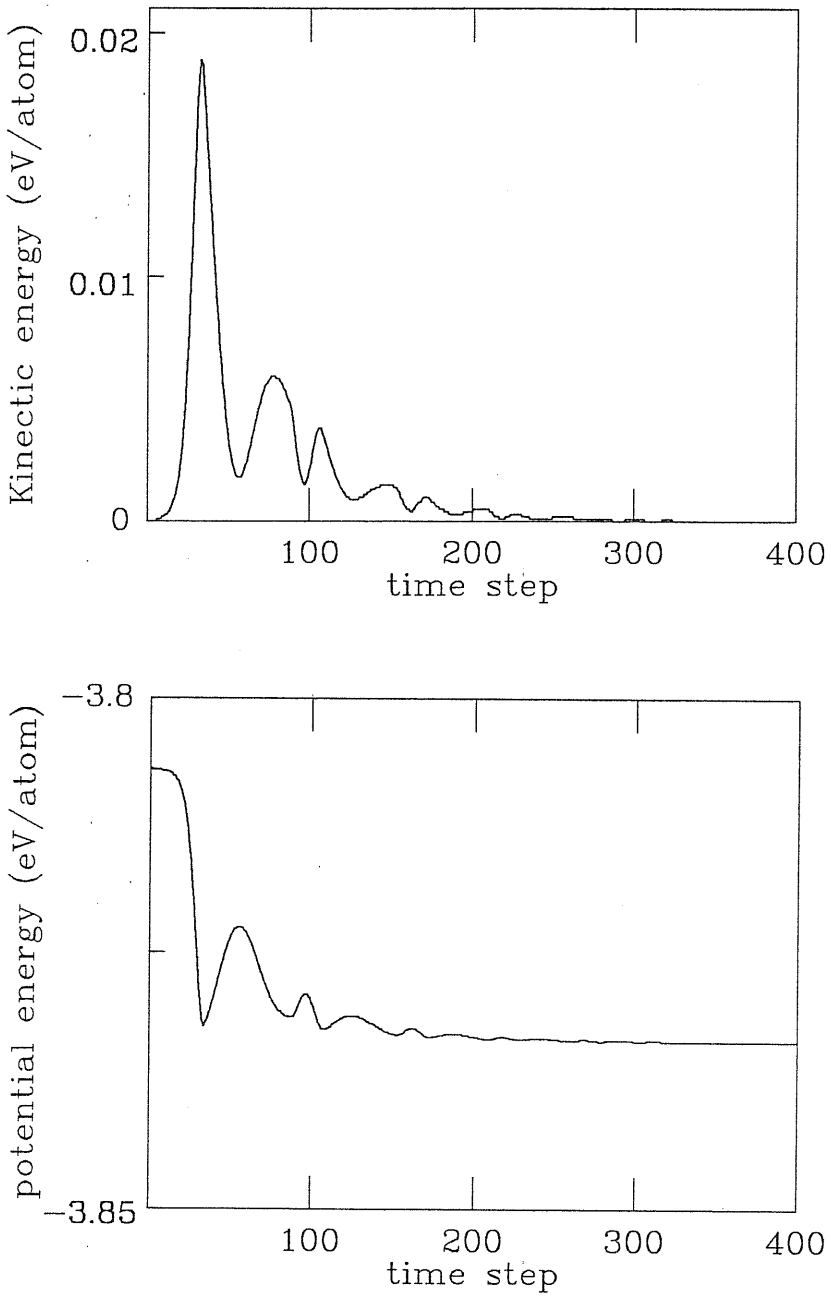

FIG. 4.2: Kinetic and potential energy as a function of time for Ge, including a split vacancy ($\xi = 0$). The system is quenched using a velocity scaling factor ($\alpha = 0.95$).

c.) Results

The results for the energetics of point defects using the Tersoff potential are presented in table 4.1 (C, Si, Ge) and table 4.2 (SiC, SiGe), in comparison with DFT-LDA calculations results (experimental data on defect energies are few and have usually rather large error bars). In table 4.2, V_j means a vacancy of element j and J_{Ti} means a J atom in a tetrahedral interstitial position surrounded by i atoms.

All the calculated defect energies in table 4.1 and table 4.2 are positive, which is of course consistent with the experimental fact that the diamond lattice is the most stable crystal structure for these semiconductors.

TAB. 4.1: Point defects energies (eV) in the diamond crystal phase of C, Si, Ge. Results of previous LDA calculations, when available, are given in brackets.

Defects	C[a]	Si[b]	Ge
vac	4.24 (7.20)	3.84 (4-5)	3.61
split vac	9.89 (9.0)	3.57 (4-5)	3.63
int(T)	19.74 (23.6)	3.62 (5-6)	8.9
int(H)	20.9	14.5 (15-16)	5.78

[a] reference[45]

[b] reference[46]

TAB. 4.2: Calculated point defects energies (eV) in the diamond crystal phase of SiC, SiGe using the stoichiometric defect combination. Results of previous LDA calculations[47], when available, are given in brackets.

defects	SiC
$V_C + V_{Si}$	7.4 (12.7)
$Si_{TC} + C_{TSi}$	21.31 (23.3)
$Si_{TSi} + C_{TC}$	22.13 (26.0)
$C_{TC} - C_{TSi}$	2.76 (2.4)

Defects	SiGe
$V_{Si} + V_{Ge}$	7.40
$Si_{TGe} + Ge_{TSi}$	7.60
$Si_{TSi} + Ge_{TGe}$	7.42
$Ge_{TGe} - Ge_{TSi}$	0.63

We also calculated the vacancy energy for different values of the reaction coordinate in order to investigate the shape of the energy barrier felt by the jumping atom, and in particular estimate the maximum energy, corresponding to a saddle point in the potential energy surface. The migration energy is then defined as the

height of the barrier:

$$E_v^{Mig} = E(S) - E(V) \tag{4.5}$$

where $E(S)$ is the energy at the saddle point and $E(V)$ is the energy with the vacancy in the equilibrium position.

In figures (4.3 a,b,c), we present the vacancy energy as a function of the reaction coordinate for Si, Ge and C. The corresponding migration energies, obtained by (4.5), are shown in table 4.3. Note that for Si the energy is referred to the split vacancy goemetry, which is the equilibrium configuration for this potential. The migration energy appears to be in qualitative agreement with LDA calculations in the case of C[48], while LDA calculations for Si suggest a much lower value of $\sim 0.3eV$[49].

TAB. 4.3: Vacancy migration energies (eV), obtained as difference of the saddle point and equilibrium energies (maximum and minimum in Fig. 4.3).

	C	Si	Ge
E_v^M	5.8	2.8	2.2

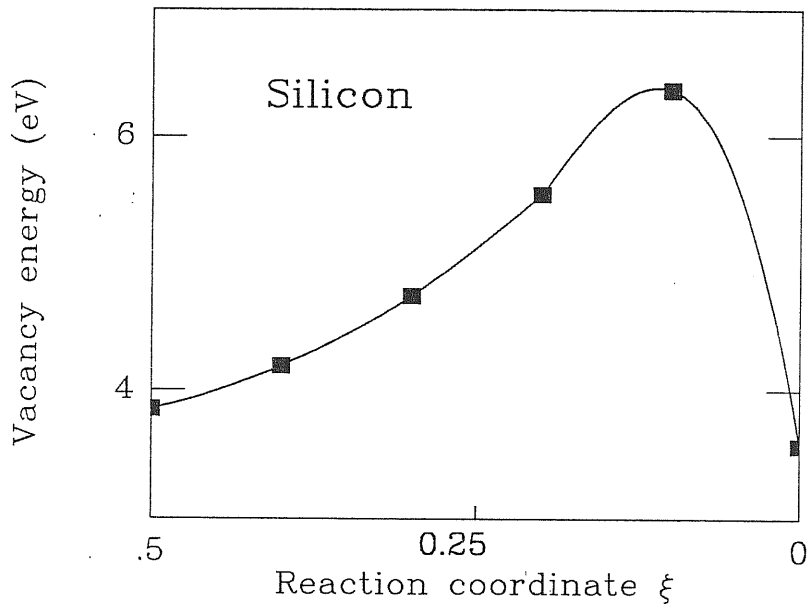

FIG. 4.3.a: Dependence of the formation energy in function of the reaction coordinate of Silicon. The square points are calculated by this theoretical model and the line is given by interpolation.

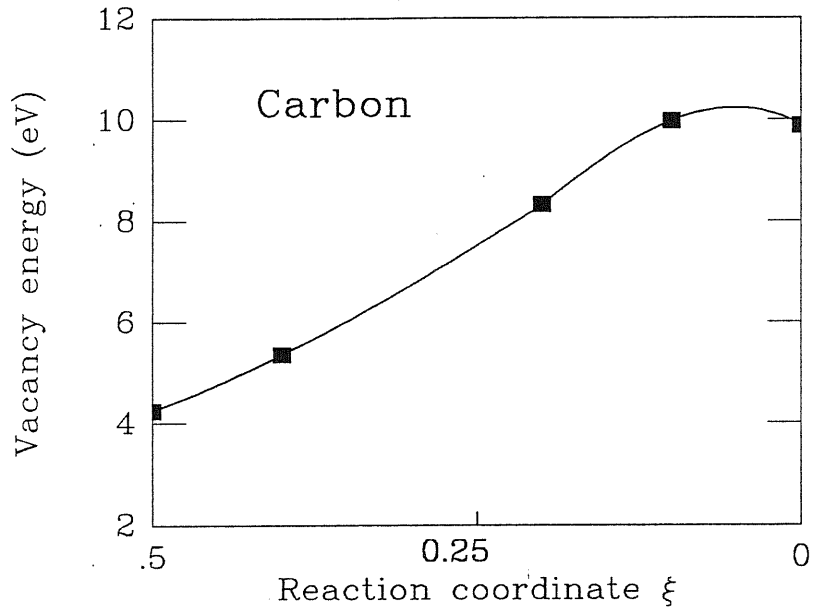

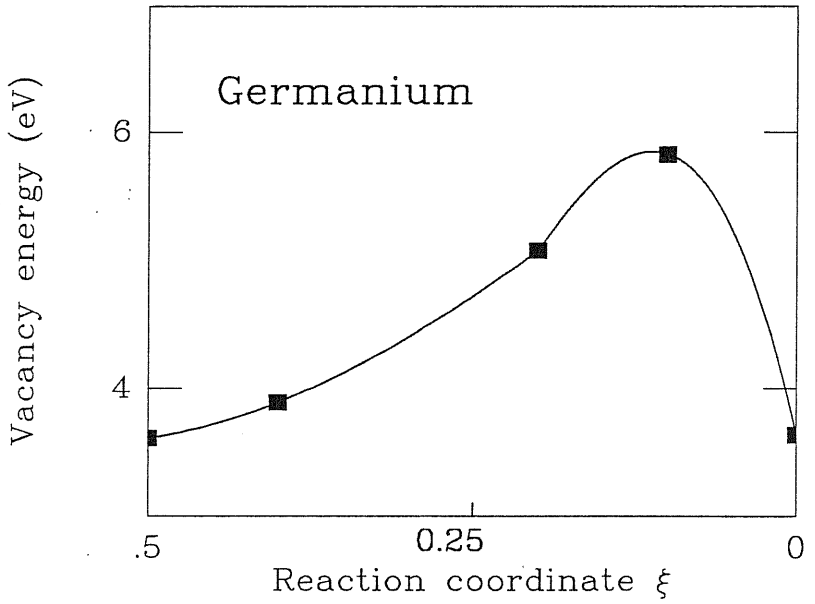

FIG. 4.3.b: Dependence of the formation energy in function of the reaction coordinate of Carbon and Germanium. The square points are calculated by this theoretical model and the line is given by interpolation.

Chapter 5

Surface Properties

It is known from experimental results that in several materials the structure of the surface atomic layer differs from that of bulk layer with the same orientation. This phenomenon is called surface reconstruction, and usually gives rise to new strange surface periodicities, often temperature–dependent. Moreover, an atomic rearrangement also takes place along the surface normal in the first, or in the first few layers. In particular, reconstruction are quite commonly observed on semiconductors surfaces, which are studied rather intensively due to their technological importance.

Surfaces are often a stringent and critical test for empirical potentials. In fact, potentials are usually constructed by fitting to bulk properties, but a surface atom experiences a local environment with a low coordination number which can be rather different from that of a bulk atom. Reconstructing surfaces are even more demanding, since they require that energy differences often very tiny should have a difined sign.

For this reason, the modeling of surface reconstructions for Si, Ge and C is an important test for the Tersoff potential. With this potential, we have studied the (100) and (111) surfaces of these materials.

a.) Reconstruction of (100) Surface

The (100) surfaces of elemental semiconductors (C, Si, Ge) are known to exhibit a 2×1 reconstruction[50]. This means, that the surface periodicity is twice as long as expected along the surface direction $[\bar{1}10]$, while it remains regular along the orthogonal $[1\bar{1}0]$ direction. The Si(100) and Ge(100) surfaces have been studied through a large number of techniques, including low–energy electron diffraction[51], angle–resolved photoemission[52], multiple–reflection infrared spectroscopy[53], all indicating a 2×1 (or 4×2) surface unit cell.

The Si(100) surface reconstruction is the subject of some controversy. Using total–energy calculations, Yin and Cohen[54] have found that buckled dimers are the lowest–energy configurations, while Pandey[55], using a more extended version of their method, has concluded that the symmetric dimer is favored. Pandey has also proposed an alternative reconstruction mechanism, a π–bonded defect structure, where a surface dimer is removed and the subsurface atoms below it are dimerized. A still different surface reconstruction, the dimer–plus–chain model, has recently been suggested by Northrup[56]. In recent experiments using the scanning tunneling microscope, Hamers, Tromp and Demuth[57] report the presence of buckled dimers, symmetric dimers, and the defect structure of Pandey on the same Si(100) surface. They do not see the dimer plus–chain reconstruction[56].

b.) Computational Method and Results

The (100) surface is modeled by a slab containing 8 layers, each including 64 atoms. We choose the x axis along the $[\bar{1}10]$ direction, the y axis along the $[1\bar{1}0]$ direction, and the z axis along the surface normal $[00\bar{1}]$. Periodic boundary conditions are imposed in the lateral (x, y) directions. The lowest three layers are held fixed, to simulate a semiinfinite crystal. For a given configuration, the surface energy σ is calculated as

$$\sigma = \frac{E_S - NE_C}{A} \tag{5.1}$$

where E_S is the total energy, E_C is the cohesion energy per atom in the bulk, N is the number of atoms and A is the slab area.

Initially, all the atoms are placed in a structure corresponding to a perfect crystal, and the surface energy is that of a perfect unreconstructed surface. Then the surface atoms, which are linked to atoms below the bulk by bonds in the $y-z$ plane, are dimerized by displacing pairs towards one another in the x direction, creating a 2×1 surface. Random velocities are given to the atoms (extracted from a Maxwellian distribution at $T = 100^oK$) and they are allowed to move under MD. The temperature is steadily reduced by quenching, permitting them to relax to the minimum energy state. A simple relaxation started from a $T = 0^oK$ sample leads to the same final state. On the other hand, run started from a perfect surface, that is without the initial preparation of an ordered superstructure of dimers, result in a rather disordered arrangement of dimers with a slightly higher energy.

We list the results in table 5.1 where we report for Si(100), Ge(100), C(100) 2×1 the relaxation energy per dimer, defined by the energy of the perfect unreconstructed surface minus the energy of the 2×1 structure, divided by the number of dimers. R_{dimer} is the separation of the dimer in the equilibrium structure. In

the figures 5.1 and 5.2 we show the final configuration of Silicon surface (the same configuration are obtained to Ge and C). Shifts from the ideal lattice positions in the above cases occur in the x and z directions only. In table 5.3 we show these shifts Δx and Δz for the atoms in the first two layers.

TAB. 5.1: Relaxation energy per dimer $E_{R_{dimer}}$ (eV) predicted by the Tersoff potential and compared with the theoretical predictions of Yin and Cohen (YC)[54], and Pandey[55].

Method	R_{dimer}	$E_{R_{dimer}}$
Si		
Present	2.30	1.52
YC	2.25	1.70
Pandey	2.22	2.06
Ge		
Present	2.50	1.17
C		
Present	1.54	1.03

TAB. 5.2: Surface energy (eV/$\AA^2$) predicted by the Tersoff potential for the 2×1 and the unrelaxed (100) surface.

Element	$E_{100_{unrel}}$	$E_{surf_{2\times1}}$
Si	0.14	0.093
Ge	0.29	0.081
C	0.48	0.40

TAB. 5.3: Shifts (in $\AA$) from the ideal lattice positions for the reconstructed (100) surface. The values in parenthesis are the results of Yin and Cohen[54]. They represent the mean value of their calculations.

	layer I	layer II
Si		
Δx	0.74 (0.81)	0.06 (0.10)
Δz	-0.19 (0.31)	0.02 (0.01)
Ge		
Δx	0.75	0.09
Δz	-0.14	0.02
C		
Δx	0.49	0.03
Δz	-0.17	0.01

FIG. 5.1: The final configurations of the atoms in the top most layer of Si(100). We can observe the 2×1 reconstruction predicted by this model.

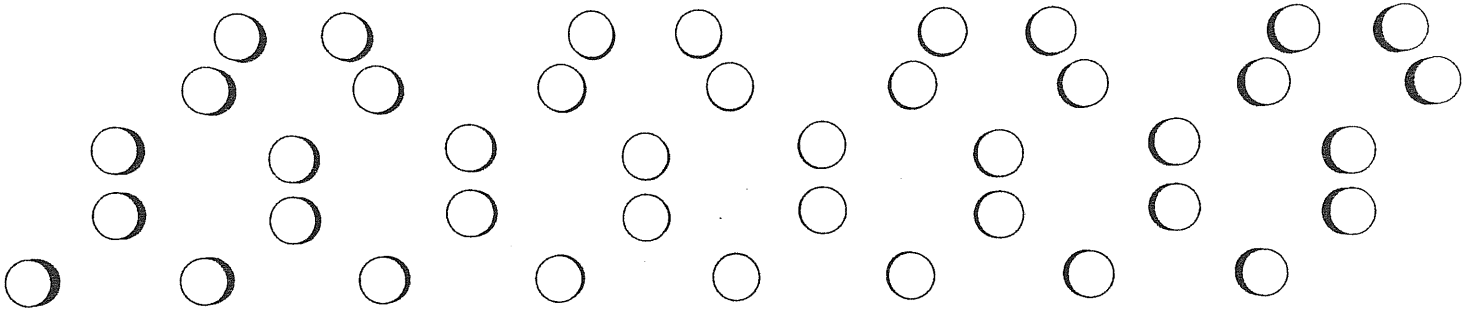

FIG. 5.2: A profile view of the final configurations of the atoms on recontructed Si(100).

c.) Reconstruction of (111) Surface

The (111) surfaces of semiconductors have been investigated by a large number of experimental studies[58]. Most of the experiments have shown that these surfaces exhibit either a 2×1 or a 7×7 superlattice structure, corresponding respectively to a metastable and a stable arrangement. Si(111) is reconstructed in the thermodynamically stable 7×7 structure at temperatures above 300^oC. when heated to 800^oC and then thermally quenched, a 1×1 phase appears, which transforms to 2×1 when the temperature is further decreased.

For Ge(111), it was experimentally observed[58] that at low temperatures (less than 300^0K) a 2×1 reconstruction takes place. It was also found that a 1×1 reconstruction is stable against heating or cooling of the cleaved crystal in the whole range $10 - 300^0K$.

Si and Ge present the same chemical properties and it is believed that their (111) surfaces should have the same atomic structure, at least for the 2×1 and 1×1 cases. Nevertheless, the models presented till now for the 2×1 structure are still controversial.

d.) Results

Different types of models are available to explain the 2×1 structure. A widely accepted model for this reconstruction is the π–bond chain model proposed by Pandey[59]. We have tested the stability of the Pandey model using the Tersoff potential, using a molecular–dynamics based on quenching strategy similar to that used for the (100) surfaces and discussed previously.

In our simulation, we have 8 layers each containing 72 atoms. The last 3 layers

are kept fixed, and periodic boundary conditions are used in the (x, y) plane. The atoms in the top two layers of the free surface of the slab were initially moved to positions close to those predicted by the π–bonded–chain model of Pandey. The relaxation procedure was subsequently performed, using a velocity factor $\alpha = 0.99$ and permitting the top five layers to relax. The system settled into a local minimum with the structure shown in figures 5.3 and 5.4 for C. Very similar pictures were obtained for Si and Ge. The surface energies of these slabs are given in table 5.4 together with the surface energy of the unrecontructed surface.

TAB. 5.4: Surface energy for the unrecontructed surface (E_{unrec}), the 2×1 π–chain model ($E_{\pi-chain}$) and the unreconstructed but relaxed (111) surface energy $E_{(111)}$ of Si, Ge and C, in (eV/$\mathring{A}^2$). R_{chain} is the distance between the atoms in the π–bonded chain running along the top of the surface.

element	E_{unrec}	$E_{(111)}$	$E_{\pi-chain}$	R_{dimer}
Si	0.080	0.074	0.13	2.25
Ge	0.070	0.066	0.13	2.01
C	0.251	0.178	0.12	1.46

The results obtained using this potential show that for Si and Ge the π–bonded–chain model for the 2×1 reconstruction corresponds to a metastable local minimum, but is not the most stable structure. On the other hand for C (figs. 5.3 and 5.4) the Pandey model corresponds to stable configuration.

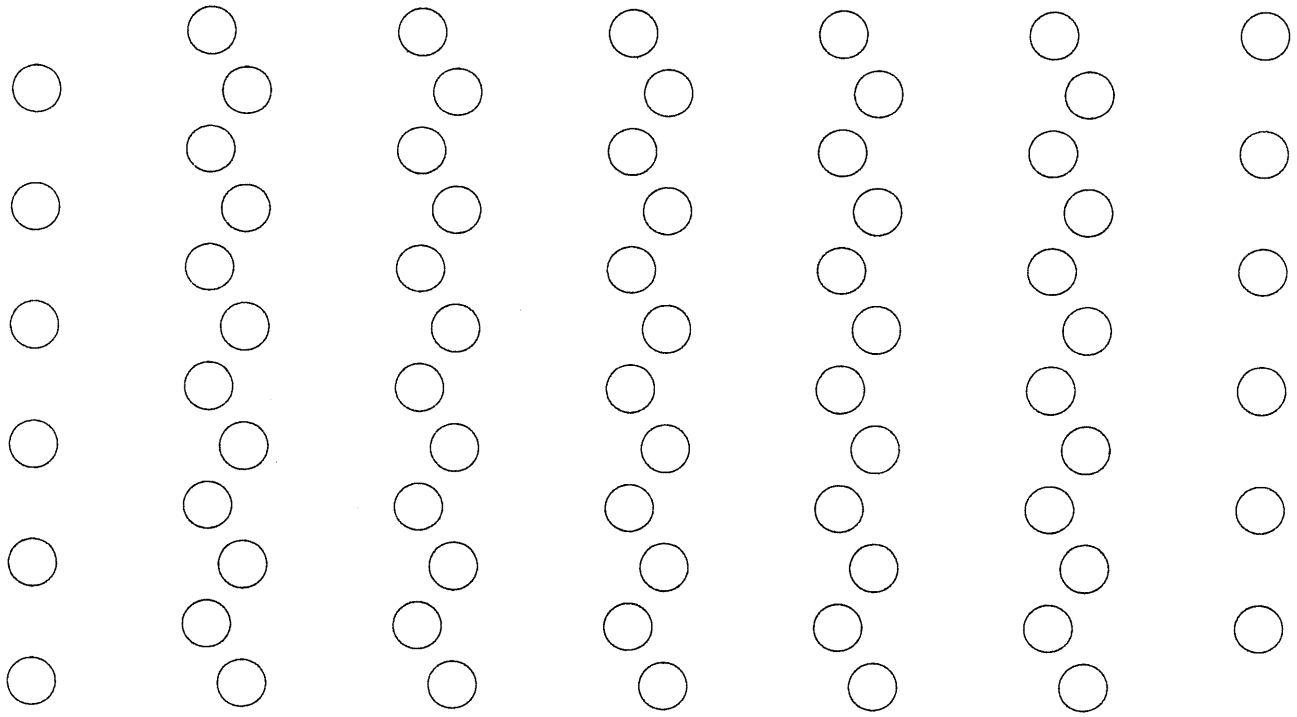

FIG. 5.3: Top view of the final configuration of the atoms on C(111). We can observe the π–bonded–chain model reconstruction predicted by Pandey.

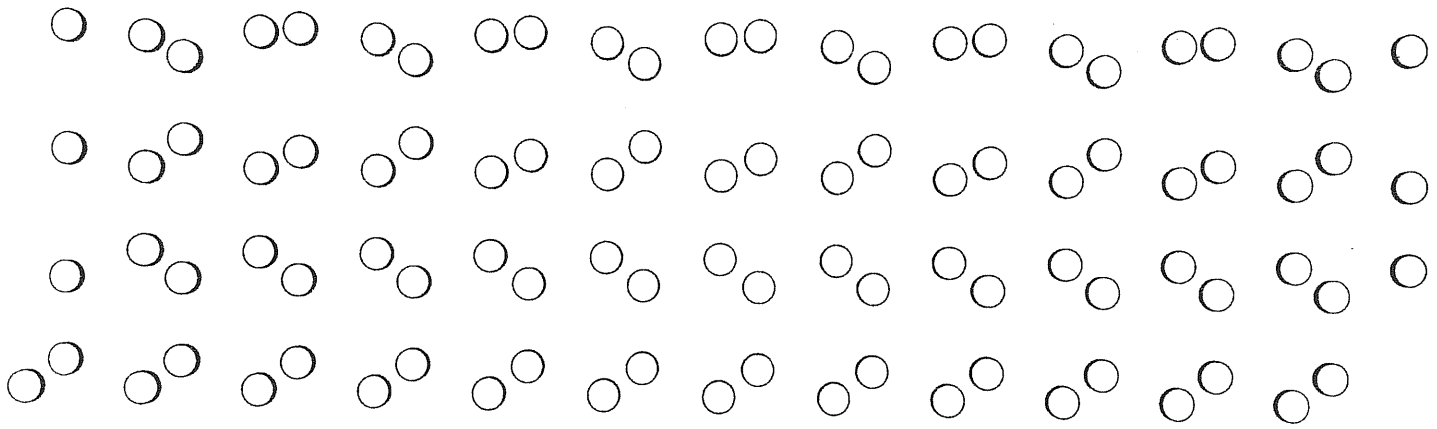

FIG. 5.4: Lateral view of the final configuration for the atoms on C(111).

Chapter 6

Conclusions

The modelling of semiconductor materials, whose main feature is the strongly directional character of covalent bonding, represents a well-known challenge for solid state physicists. In spite of recent developments of ab-initio methods for computer simulation of semiconductors, schemes based on empirical, classical potentials are still of interest when the necessity arises to study phenomena involving relatively large number of particles (e.g., $N > 100$), or long simulation times. This is the case for many problems of scientific and technological interest such as, for example, surface reconstruction, crystal growth, self-diffusion. The purpose of this work was to investigate the behaviour of a family of state-of-the-art classical potentials for semiconductors (C, Si, Ge and their mixtures), made by Tersoff.

First of all, bulk properties have been considered. A study of the energy as a function of the atomic volume for various crystalline structures shows that, as expected, the diamond structure is the most stable at low pressures. However, Si and Ge are found to transform at high pressure to the b.c.c. phase, instead of the β-tin structure as experimentally observed.

A study of the bulk phonon spectrum in the diamond structure shows a good agreement with experimental data as far as the longitudinal acoustic modes are concerned, while the frequencies of optical and transverse acoustic modes are slightly overestimated.

In order to proceed with the study of the structure and energetics of defects and surfaces, a molecular dynamics program with forces derived by Tersoff poten-

tials has been implemented. Although used here primarily as a tool for energy minimization, this program constitutes a valid and general instrument for studies at finite temperature and in low-symmetry conditions, which may constitute the subject of future work.

Formation energies of defects and interstitials are found to be in fair agreement with the more accurate results obtained from DFT-LDA calculations. However, in Si and Ge the vacancy migration energy is far too high, and therefore the self-diffusion coefficient is severely underestimated. The potential for C appears to be more realistic with respect to point defect properties.

An application of Tersoff potentials to the structure of low-index surfaces, known to reconstruct in semiconductors, shows a quite acceptable description of the 2×1 reconstruction of (100) surfaces. On the other hand, with again the notable exception of the C potential, the Pandey model for the 2×1 reconstruction of (111) surfaces appears to be higher in energy than the non-reconstructed surface, quite in contrast with the most recent suggestions and experiments on the structure of Si(111).

Even if somewhat inaccurate in some areas, these potentials constitute a clear advance in semiconductor modelling. Their analytical form, based on a many-body term where coordination plays a key role, is certainly closer to the physics of semiconductors than the simple three-body terms typical of the potentials of the previous generation. Moreover, their applicability to mixtures as well as to the pure elements, exploited in some of the calculations presented in this thesis, is a clear advantage. It is therefore likely that future, more refined potentials for semiconductors, hopefully able to overcome the weaknesses found and described here, will naturally evolve from Tersoff's work.

Appendix A

Calculation of the force

The force is given by equation (4.1). Here we use the same variable names that we use in the text.

The Tersoff potential depends on two sets of variables $\{R_{ij}\}$ and $\{cos(\theta_{ijk})\}$ where the subindices represent all the particles in the system. Therefore, with the application of the chain rule, we obtain

$$\frac{\partial E}{\partial \mathbf{R}_n} = \frac{1}{4}\sum_{i\neq j}\sum_{l\neq m}\frac{\partial V_{lm}}{\partial R_{ij}}\frac{\partial R_{ij}}{\partial \mathbf{R}_n} + \frac{1}{4}\sum_{i\neq j\neq k}\sum_{l\neq m}\frac{\partial V_{lm}}{\partial cos(\theta_{ijk})}\frac{\partial cos(\theta_{ijk})}{\partial \mathbf{R}_n} \qquad (A.1)$$

the factor $\frac{1}{4}$ in the first term of equation (A.1) is due to the fact in the summation it is counted two times as it does not distinguish $i \rightarrow j$ and $j \rightarrow i$ also to l, m. In the second term of the equation the factor $\frac{1}{4}$ is counted two times because the potential occupies a preferential position in i and the changes from $j \rightarrow k$ and $k \rightarrow j$ oblige to count it double (it is considered implicitly the factor $\frac{1}{2}$ because it doesnot distinguish between the change of l, m in the potential). We want to underline that in this notation about equation (A.1) the sums run over all values of i, j, k everyone different from each other.

The derivatives of R_{ij} and $cos(\theta_{ijk})$ with respect to $\mathbf{R}_n$ are

$$\frac{\partial R_{ij}}{\partial \mathbf{R}_n} = \frac{\mathbf{R}_{ij}}{R_{ij}}(\delta_{in} - \delta_{jn}) \qquad (A.2)$$

and

$$\frac{\partial cos(\theta_{ijk})}{\partial \mathbf{R}_n} = \left(\frac{\mathbf{R}_{ij} + \mathbf{R}_{ik}}{R_{ij}R_{ik}} - \frac{\mathbf{R}_{ij} \cdot \mathbf{R}_{ik}}{R_{ik}R_{ij}^3}\mathbf{R}_{ij} - \frac{\mathbf{R}_{ik} \cdot \mathbf{R}_{ij}}{R_{ij}R_{ik}^3}\mathbf{R}_{ik} \right) \delta_{in} +$$

$$\left(\frac{\mathbf{R}_{ij} \cdot \mathbf{R}_{ik}}{R_{ik}R_{ij}^3}\mathbf{R}_{ij} - \frac{\mathbf{R}_{ik}}{R_{ij}R_{ik}} \right) \delta_{jn} + \left(\frac{\mathbf{R}_{ik} \cdot \mathbf{R}_{ij}}{R_{ij}R_{ik}^3}\mathbf{R}_{ik} - \frac{\mathbf{R}_{ij}}{R_{ik}R_{ij}} \right) \delta_{kn} \qquad (A.3)$$

where δ_{lm} is the Kroneker delta defined as

$$\delta_{lm} = \begin{cases} 1, & \text{if } l = m \\ 0, & \text{otherwise.} \end{cases} \qquad (A.4)$$

Through the calculation of the simple derivations of the potential, cancelling the summations by deltas of Kroneker and having in mind that the b_{ij} in the equation 2.4, is asymmetric ($b_{ij} \neq b_{ji}$) in the equation (A.1), we obtain the following expressions

$$\frac{\partial E}{\partial \mathbf{R}_n} = \frac{1}{2} \sum_{j \neq n} \dot{f}_C(R_{nj}) \left[2 f_R(R_{nj}) + f_A(b_{nj} + b_{jn}) \right] \quad +$$

$$f_C(R_{nj}) \left[2\dot{f}_R(R_{nj}) + \dot{f}_A(R_{nj})(b_{nj} + b_{jn}) \right] \frac{\mathbf{R}_{nj}}{R_{nj}} \quad + \qquad (A.5.a)$$

$$\frac{1}{2} \sum_{j \neq k \neq n} \dot{f}_C(R_{nj}) \left[f_A(R_{nk}) f_C(R_{nk}) g(cos(\theta_{njk})) A_{nk} \right. \quad +$$

$$\left. f_A(R_{jk}) f_C(R_{jk}) g(cos(\theta_{jnk})) A_{jk} \right] \frac{\mathbf{R}_{nj}}{R_{nj}} \quad + (A.5.b)$$

$$\frac{1}{2} \sum_{j \neq k \neq n} f_C(R_{nj}) f_C(R_{nk}) \dot{g}(cos(\theta_{njk})) \left[f_A(R_{nj}) A_{nj} \right. \quad +$$

$$\left. f_A(R_{nk}) A_{nk} \right] \left(1 - \frac{\mathbf{R}_{nj}.\mathbf{R}_{nk}}{R_{nj}^2} \right) \frac{\mathbf{R}_{nj}}{R_{nj}R_{nk}} \quad + \qquad (A.5.c)$$

$$\frac{1}{2} \sum_{i \neq k \neq n} f_C(R_{ni}) f_C(R_{ik}) \dot{g}(cos(\theta_{ink})) \left[f_A(R_{ni}) A_{in} \right. \quad +$$

$$f_A(R_{ik})A_{ik})]\left(\frac{\mathbf{R}_{in}.\mathbf{R}_{ik}}{R_{in}^2}\mathbf{R}_{in}-\mathbf{R}_{ik}\right)\frac{1}{R_{ni}R_{ik}} \qquad (A.5.d)$$

these expressions can be simplified taking into account that the vectors $\mathbf{R}_{nk}$ can be written as

$$\mathbf{R}_{nk}=\mathbf{R}_{nj}+\mathbf{R}_{jk}$$

and

$$\mathbf{R}_{nk}.\mathbf{R}_{nk}=R_{nj}^2+\mathbf{R}_{nj}.\mathbf{R}_{jk}$$

Then, we have the following equality:

$$1-\frac{\mathbf{R}_{nj}.\mathbf{R}_{nk}}{R_{nj}^2}=-\frac{\mathbf{R}_{nj}.\mathbf{R}_{jk}}{R_{nj}}=cos(\theta_{jnk})\frac{R_{jk}}{R_{nj}}$$

so equations (5.c) and (5.d) become

$$\frac{1}{2}\sum_{j\neq k\neq n} f_C(R_{nj})f_C(R_{nk})\dot{g}(cos(\theta_{njk}))\,[f_A(R_{nj})A_{nj} \quad +$$

$$f_A(R_{nk})A_{nk})]\}\,cos(\theta_{jnk})\frac{R_{jk}}{R_{nj}^2}\mathbf{R}_{nj} \qquad (A.6.a)$$

$$-\frac{1}{2}\sum_{j\neq k\neq n}\frac{f_C(R_{nj})}{R_{nj}}f_C(R_{jk})\dot{g}(cos(\theta_{ink}))\,[f_A(R_{nj})A_{jn}\,+$$

$$f_A(R_{jk})A_{jk})]\left(cos(\theta_{jkn})\frac{\mathbf{R}_{nj}}{R_{nj}}+\frac{\mathbf{R}_{jk}}{R_{jk}}\right)\Bigg\} \qquad (A.6.b)$$

where in all the equations the sum runs over all values of i and k different from n and different among themselves, i.e :

$$\sum_{i\neq k\neq n}=\sum_{i\neq k}\sum_{k\neq n}$$

and $\dot{f}(x)$ represents the derivation of the function with respect to the argument x : $\frac{df}{dx}$. The new function A_{lm} that appears in these calculations is defined as

$$A_{lm}=-\frac{\chi_{lm}}{2}\left(1+\beta_l^{n_l}\zeta_{lm}^{n_l}\right)^{-1/2n_l-1}\beta_l^{n_l}\zeta_{lm}^{n_l-1}$$

The set of equations $(5.a), (5.b), (6.a)$ and $(6.b)$ gives the solution of the equation $(A.1)$ and by changing the sign we obtain the value of the vector force for a specified particle.

It is known that for the calculation of the force in molecular dynamics programs a very long time is required, because this force is necessary for the movements of all the particles of the system. In this way this force must be minimized, which means using less time as possible in the calculation of each particle. With this purpose for Tersoff potential in our program we employed one loop for each particle. So we could avoid calculating two times or three times the same functions. All the functions are computed explicitly in the calculation of the force. Moreover b_{ij}, A_{lm}, and ζ were previously calculated in the possible range of values they can have. The values of the $\cos(\theta_{ijk})$ were calculated only once explicitly in the force. At the begining of this program, all the parameters which specified the particular component or multicomponents, like C, Si, Ge, SiC and SiGe were calculated in order to avoid calculating the square root for the evaluation of every function.

It was in this way that it was possible to compute the force of each particle with this type of potential spending a minimum time and optimizing this program of molecular dynamics valid for simple component like C, Si, and Ge or multicomponents like SiC and SiGe because it makes a distinction for every single particle.

Bibliography

[1] R. Car and M. Parrinello, Phys. Rev. Lett. 55,2471 (1985)

[2] J. Tersoff, Phys. Rev. B 38,5566 (1989)

[3] J. Tersoff, Phys. Rev. B 37,6991 (1988), Phys. Rev. B 38,9902 (1988)

[4] J. Tersoff, Phys. Rev. Lett. 61,2879 (1988)

[5] T. N. Keating, Phys. Rev. 145,637 (1966)

[6] A review of such aproach has been given by E. O. Kane Phys. Rev. B 31,7865 (1985)

[7] E. Pearson, T. Takai, T. Halicioglu and W. A. Tiller, J. Cryst. Growth 70,33 (1984), T. Takai, T. Halicioglu and W. A. Tiller, Scr. Metal. 19,709 (1985)

[8] B. M. Axilrod and E. Teller, J. Chem. Phys. 11,299 (1943)

[9] F. Stillinger and T. A. Weber, Phys. Rev. B 31,5262 (1985)

[10] B. W. Dondson, Phys. Rev. B 33,7361 (1986)

[11] U. Landam, W. D. Luedtke, R. N. Bannett, C. L. Cleveland, M. W. Ribarsky, E. Arnold, S. Ramseh, H. Baumgart, A. Martinez and B. Khan, Phys. Rev. Lett. 56,155 (1986)

[12] B. W. Dondson and P. A. Taylor, App. Phys. Lett. 49,642 (1986)

[13] R. Biswas and D. R. Hamann, Phys. Rev. Lett. 55,2001 (1985)

[14] J. H. Rose, J. R. Smith, F. Guinea and J. Ferrante, Phys. Rev. B 29,2963 (1984)

[15] B. W. Dodson Phys. Rev. B 35,2619 (1987)

[16] G. C. Abell, Phys. Rev. B 31,6184 (1985)

[17] R. Biswas and D. R. Hamann, Phys. Rev. B 36,6434 (1987)

[18] M. T. Yin and M. L. Cohen, Phys. Rev. B. 26,3259 (1982)

[19] I. Kwon, R. Biswas, G. R. Grest, C. M. Soukoulis, Phys. Rev. B 41,3678 (1990)

[20] P. C. Kelires and J. Tersoff, Phys. Rev. Lett. 63,1164 (1989)

[21] P. C. Kelires and J. Tersoff, Phys. Rev. Lett. 61,562 (1988)

[22] B. W. Dondson, Phys. Rev. B 35,2795 (1987)

[23] B. C. Bolding and H. C. Andersen, Phys. Rev. B 41,10568 (1990)

[24] J. Chelikowsky, Phys. Rev. Lett. 60,2669 (1988); J. Chelikowsky, J. C. Phillips, M. Kamal and M. Strauss, Phys. Rev. Lett. 62,292 (1989)

[25] H. Wang and R. Messmer unpublished report

[26] J. Chelikowsky and J. C. Phillips, Phys. Rev. Lett. 63,1653 (1989)

[27] K. E. Khor and S. Das Sarma, Phys. Rev. B 38,3318 (1988), Phys. Rev. B 39,1188 (1989)

[28] M. I. Baskes, Phys. Rev. Lett. 59,2666 (1987)

[29] M. S. Daw and M. I. Baskes, Phys. Rev. Lett. 50,1285 (1983), Phys. Rev. B 29,6443 (1984)

[30] M. Born and K. H. Huang, *Dynamical Theory of Crystal Lattices* (Oxford University, NewYork 1954)

[31] L. Guttman and J. A. Rothstein, Phys. Rev. B 19,6062 (1979)

[32] F. P. Bundy, J. Geophys. Res. 85,6930 (1980); J. E. Field *The Properties of Diamond*(Academ. London 1979)

[33] Y. K. Vohra, K. E. Brister, S. Desgreniers, A. L. Ruoff, K. J. Chang and M. L. Cohen, Phys. Rev. Lett. 56,1944 (1986)

[34] K. J. Chang and M. L. Cohen, Phys. Rev. B 35,8196 (1987)

[35] J. L. Martin and A. Zunger, Phys. Rev. Lett. 56,1400 (1986)

[36] Pasquale Pavone, Magister Thesis SISSA-1989

[37] O. Jepsen and O. K. Andersen, Solid state commun. 9,1763 (1971)

[38] H. L. Skriver *The LMTO Method* Springer Verlag (1984)

[39] J. L. Warren and J. L. Yarnell, Phys. Rev. 158,805 (1967)

[40] G. Dolling, in *Inelastic Scattering of Neutrons in Solids and Liquids* IAEA, Viena 1963 Vol. II, pag 37; G. Nilsson and G. Nelin, Phys. Rev. B 6,3777 (1972)

[41] G. Nilsson and G. Nelin, Phys. Rev. B 3,364 (1971)

[42] T. Allen and Tildesley, *Computer simulation of liquids* (Cambrige University, 1986)

[43] Furio Ercolessi, Computer program about cell method, 1986

[44] C. H. Bennett *Diffusion in Solid* Edits. by A. S. Nowick and J. J. Burton (1975)

[45] J. Bernholc, A. Antonelli, T. M. Del Sole, Y. Bar-Yam and S. T. Pantelides, Phys. Rev. Lett. 61,2689 (1988)

[46] R. Car, P. J. Kelly, A. Oshiyama and S. T. Pantelides, Phys. Rev. Lett. 52,1814 (1984); 54,360 (1985); G. A. Baraff and M. Schllueter Phys. Rev. B 30,3460 (1984); Y. Bar-Yam and J. D. Joannopoulus, ibid. 30,1844 (1984)

[47] J. Bernholc, A. Antonelli, C. Wang, and R. F. Davis, in *Proceeding of the Fifteenth International Conference on Defects in Semiconductors*, Budapes,

Hungaria, 1988 (unpublished)

[48] J. Bernholc, A. Antonelli, T. M. Del Sole, Y. Bar–Yam, and S. T. Pantelides, Phys. Rev. Lett. 61,2689 (1988).

[49] E. Smargiassi, PhD Thesis SISSA-1990

[50] J. C. Phillips, Surf. Sci. 40,459 (1973); R. E. Schlier and H. E. Farnsworth, *Semiconductor Surface Physics*(Univ. of Pennsylvania Press, Philadelphis 1957)

[51] W. Monch, Surf. Sci. 63,79 (1977)

[52] H. D. Hagstrum and G. E. Becker, Phys. Rev. B 8,1580 (1973)

[53] J. J. Lander, Prog. Solid State Chem. 2,26 (1965)

[54] M. T. Yin and M. L. Cohen, Phys. Rev. B 26,5668 (1982)

[55] K. C. Pandey in *Proceeding of the Seventeenth International Conference of the Physics Semiconductors* Edited by D. J. Chadi and W. A. Harrison (Springer-NewYork 1985)

[56] J. E. Northrup, Phys. Rev. Lett. 54,815 (1985)

[57] R. M. Hamers, R. J. Tromp and J. E. Demuth, Phys. Rev. Lett. 55,1303 (1985)

[58] V. A. Grazhulis in *Proceeding of the Seventeenth International Conference of the Physics Semiconductors* Edited by D. J. Chadi and W. A. Harrison (Springer-NewYork 1985)

[59] K. C. Pandey, Phys. Rev. Lett. 47,1913 (1981)